HHS Public Access

Author manuscript

J Comp Neurol. Author manuscript; available in PMC 2016 October 01.

Published in final edited form as:

J Comp Neurol. 2015 October 1; 523(14): 2138–2160. doi:10.1002/cne.23783.

Spinal cord neuron inputs to the cuneate nucleus that partially survive dorsal column lesions: a pathway that could contribute to recovery after spinal cord injury

Chia-Chi Liao[*], **Gabriella E. DiCarlo**, **Omar A. Gharbawie**, **Hui-Xin Qi**, and **Jon H. Kaas**

Department of Psychology, Vanderbilt University, Nashville, TN 37240, USA

Abstract

Dorsal column lesions at a high cervical level deprive the cuneate nucleus and much of the somatosensory system of its major cutaneous inputs. Over weeks of recovery, much of the hand representations in the contralateral cortex are reactivated. One possibility for such cortical reactivation by hand afferents is that preserved second-order spinal cord neurons reach the cuneate nucleus through pathways that circumvent the dorsal column lesions, contributing to cortical reactivation in an increasingly effective manner over time. To evaluate this possibility, we first injected anatomical tracers into the cuneate nucleus and plotted the distributions of labeled spinal cord neurons and fibers in control monkeys. Large numbers of neurons in the dorsal horn of the cervical spinal cord were labeled, especially unilaterally in lamina IV. Labeled fibers were distributed in the cuneate fasciculus and lateral funiculus. In three other squirrel monkeys, unilateral dorsal column lesions were placed at the cervical segment 4 (C4) level and tracers were injected into the ipsilateral cuneate nucleus. Two weeks later, a largely unresponsive hand representation in contralateral somatosensory cortex confirmed the effectiveness of the dorsal column lesion. However, tracer injections in the cuneate nucleus labeled only about 5% of the normal number of dorsal horn neurons, mainly in lamina IV, below the level of lesions. Our results revealed a small second-order pathway to the cuneate nucleus that survives high cervical dorsal column lesions by traveling in the lateral funiculus. This could be important for cortical reactivation by hand afferents, and recovery of hand use.

Keywords

second-order spinal cord pathway; cuneate nucleus; dorsal column lesion; cortical reactivation; lateral funiculus

[*]Corresponding author: Name: Chia-Chi Liao, Address: 301 Wilson Hall, Department of Psychology, Vanderbilt University, 111 21st Avenue South, Nashville, TN 37240, Phone: +1-615-322-5132, Fax: +1-615-343-8449, chia-chi.liao@vanderbilt.edu.

Conflict of interest statement: The authors have no conflict of interest.

Role of authors: Study concept and design: C.C.L., H.X.Q., J.H.K. Acquisition of data: C.C.L., G.E.D, O.A.G., H.X.Q. Analysis and interpretation of data: C.C.L., G.E.D, H.X.Q., J.H.K. Drafting of the article: C.C.L., J.H.K. Obtained funding: O.A.G, H.X.Q., J.H.K.

Introduction

Lesions of dorsal columns at a high cervical level of the spinal cord in monkeys remove the direct peripheral inputs from the hand to the cuneate nucleus, and consequently inactivate much of the entire somatosensory system (see reviews in Kaas et al., 2008; Qi et al., 2014a). Over weeks to months of recovery, much of the deactivated somatosensory cortex becomes responsive to touch (Bowes et al., 2013; Chen et al., 2012; Jain et al., 1997; Qi et al., 2011a) in parallel with the restoration of skilled hand use (Qi et al., 2013). One possibility for the reactivation of hand cortex is that incomplete dorsal column lesions spare a few inputs from the hand that project to the cuneate nucleus through the dorsal columns. However, reactivation is evident in hand cortex even after complete or nearly complete dorsal column lesions (Qi et al., 2011a). Thus, other possible sources of cortical reactivation by inputs from the hand need to be considered.

Another possibility is that second-order neurons in the dorsal horn of the spinal cord that receive inputs from afferents from the hand project to the cuneate nucleus and become increasingly effective in activating cuneate nucleus neurons over weeks to months of recovery after dorsal column lesions. Such second-order neurons are known to exist in the dorsal horn of the spinal cord of monkeys (Cliffer and Willis, 1994; Rustioni et al., 1979) and other mammals (Dick et al., 2001; Giesler et al., 1984; Rustioni, 1974). The course of this second order pathway to the cuneate nucleus appears to largely involve the cuneate fasciculus, although some axons may traverse laterally in the lateral funiculus (Cliffer and Giesler, 1989; Enevoldson and Gordon, 1989b; Rustioni et al., 1979). While many of these second-order inputs may respond to touch on the hand (Dick et al., 2001), their receptive field properties and functions in primates are not well understood.

In the experiments described here, we injected retrograde tracers into the hand representations of the cuneate nucleus of control squirrel and owl monkeys to reveal the normal distribution of spinal cord neurons that project to the cuneate nucleus. In a separate group of squirrel monkeys, we injected tracers into the hand representation of the cuneate nucleus immediately after an extensive lesion of the dorsal columns at a high cervical level of the spinal cord. Two weeks after lesion, we mapped the receptive fields of the hand in the area 3b contralateral to the lesion side using microelectrode recordings. Our results indicate that few projections of second-order neurons, approximately 5%, below the level of the lesions remain, and that hand cortex is unresponsive two weeks after complete lesions. Yet, remaining spinal cord inputs may become capable of driving cuneate nucleus neurons over longer recovery times to become an important source of cortical reactivation after the peripheral nerve afferents to the cuneate nucleus have been lost.

Materials and Methods

The primary objective of the present study was to determine if alternative spinal cord pathways traveling outside the dorsal column could potentially contribute to the reactivation of the somatosensory system and recovery of hand use after dorsal column lesions. We first established the connectional organization of spinocuneate pathways, including the laminar origins of projecting neurons in the spinal cord and the ascending routes, in two control

squirrel monkeys (*Saimiri bolivian*) and one control owl monkey (*Aotus nancymaae*). The remaining projections to the cuneate nucleus from neurons in the spinal cord after dorsal column lesions at a high cervical level were studied in three additional squirrel monkeys. All surgical procedures and animal care were conducted in accordance with the *Guide for the Care and Use of Laboratory Animals* by the National Institutes of Health and approved by the Animal Care and Use Committee of Vanderbilt University.

Microelectrode multiunit mapping and tracer injections in the cuneate nucleus

In preparation for microelectrode mapping and tracer injections, monkeys were initially tranquilized with an intramuscular injection (IM) of ketamine hydrochloride (10–25 mg/kg, IM) and the anesthesia was continued by an inhaled anesthesia, isoflurane (1–2% mixed in O_2). While fully anesthetized, monkeys were placed in a stereotaxic frame, and the head was rotated ventrally to expose the base of skull near the foramen magnum. Exposures of the cervical spinal cord and cuneate nucleus were performed under aseptic conditions. Vital signs including heart rate, respiration rate, blood temperature, expiration CO_2, arterial O_2 saturation and body temperature were monitored every 10 min throughout the procedure. An incision was made in the skin at the midline over the back of head and extended caudally to upper vertebrae C5. Muscle tissues overlying the junction of the skull with the spinal vertebrae were retracted. A portion of the upper cervical spinal cord (C3–C5) was exposed and dura was cut and displaced to provide access for microelectrode penetrations and tracer injections.

Multiunit microelectrode mapping—Previous electrophysiological recordings in the cuneate nucleus (Xu and Wall, 1999) and studies of primary projections from the hand to the cuneate nucleus (Florence et al., 1991) in squirrel monkeys guided our placement of microelectrodes for somatotopic mapping. Low-impedance tungsten microelectrodes (1 MΩ) were inserted perpendicularly into the cuneate nucleus, which is located 1–2 mm lateral to the midline and extends to a depth of approximately 1500 μm. Neuronal receptive fields for multiunit recording sites were systematically determined every 300 μm (depth) along a recording site until no responses to touches on the body surface were detected. Standard mapping methods (Qi et al., 2011a) such as lightly touching the skin with fine probes, brushing hair, tapping the skin and manipulating muscles or joints, were used to identify receptive fields and neuronal responsive modalities.

Tracer injections—To ensure that tracers were confined to cuneate nucleus, we injected tracers in the center of the electrophysiologically defined hand representation. Three neuroanatomical tracers were injected with 1-μl or 2-μl Hamilton syringes that had a glass pipette drawn to a fine tip attached. Tracers included 0.05–1.0 μl of 1% cholera toxin subunit B (CTB; Sigma, St. Louis, MO) in distilled water, or 0.05–0.1 μl of 10% fluoro-ruby (FR, MW 3,000 and 10,000 mixture; Invitrogen, Carlsbad, CA) or 0.05–0.1 μl of 10% biotinylated dextran amine (BDA, MW 3,000 and 10,000 mixture; Invitrogen) in pH 7.4 phosphate buffer. CTB was used to retrogradely label cell bodies, whereas FR and BDA were used to trace spinal axons that connect with the cuneate nucleus. In owl monkey 11–18, CTB was injected into the hand representation in cuneate nucleus on the left side and also into the gracile nucleus on the right side. In the other five cases, CTB was injected

unilaterally into the hand representation of cuneate nucleus. For each injection site, the tracer was first delivered at a depth of 800 μm, and a second injection was placed at 600 μm. Micropipettes were kept in position for 2 and 5 minutes respectively after each injection to minimize backflow. After the syringes were withdrawn, the cut dura was replaced, and the opening was covered by a piece of Gelfilm and Gelfoam before it was closed. Each monkey's recovery from anesthesia was closely monitored. Analgesics and antibiotics were given every 12 hours for 3 consecutive days.

Unilateral dorsal column lesion

We intended to completely interrupt dorsal column fibers at a high cervical level to remove direct peripheral inputs from the hand. Three squirrel monkeys received a unilateral dorsal column lesion at C4 immediately after tracer injections in the ipsilateral cuneate nucleus. We retracted the muscles covering C3–C5 and removed the dorsal arch of the C4 vertebrae. After the dura and pia were retracted, the dorsal column was cut with a pair of iris surgical scissors in two cases (SqM 12–52 and SqM 13-01). In squirrel monkey 13–17, we used fine tipped forceps to crush the dorsal column at the cervical level C4 for one minute, followed by a cut with surgical scissors in the same location. In each case, the dura was replaced, the opening was covered by a piece of Gelfilm and Gelfoam, and the opening was closed.

Subcutaneous digit injection

To determine the completeness of the dorsal column lesions, we injected a transganglionic tracer, choleratoxin subunit B conjugated with wheat germ agglutinin-horseradish peroxide (B-HRP, 0.2% in distilled H_2O, List Biological Labs, Campbell, C), into digits of both hands in monkeys that received dorsal column lesions. To allow for tracer transport time, these injections were placed 5 days before the terminal mapping procedure. The results allowed us to later compare the areas of labeled axon terminals in the left and right cuneate nuclei that received control or interrupted dorsal column inputs, as a measure of the completeness of the dorsal column lesions (Qi et al., 2011a). In preparation for the injection, each monkey was tranquilized with ketamine hydrochloride (10mg/kg, IM), and transitioned to an inhalation of isoflurane (1–2%) in oxygen. While anesthesia was at a surgical level, subcutaneous injections of 5 μl of B-HRP solution with a Hamilton syringe were made into the distal parts of glabrous digits 1, 3 and 5 of both hands, and the monkeys were monitored during recovery from anesthesia.

Multiunit microelectrode mapping in area 3b

Procedures followed those previously described (Qi et al., 2011a). We mapped the hand representation of area 3b in the contralateral primary somatosensory cortex two weeks after dorsal column lesions to see if neurons in the hand representation were deactivated by the interruption of the dorsal column fibers, thereby providing evidence on the effectiveness of the dorsal column lesions. Since inputs from the trigeminal nucleus were not affected by the dorsal column lesions, we mapped the face representation as a positive control. The neuronal responsiveness from face cortex was compared to that obtained from the hand cortex. In preparation for surgery, monkeys were initially tranquilized with ketamine hydrochloride (10mg/kg, IM) followed by an inhalation of isoflurane (1–2%), and placed in a stereotaxic head-holder. The anesthesia was then transitioned to an intravenous administration of

ketamine hydrochloride (12 mg/kg/hr). Vital signs were monitored throughout the procedures. Unilateral craniotomies contralateral to the dorsal column lesion side were made over parietal cortex to expose the representations of hand and face. Recordings were obtained with low-impedance tungsten microelectrodes (1 MΩ) that were lowered perpendicularly through the cortical surface to the depth of 650 μm where the middle layers of cortex were located. We systematically spaced the microelectrode penetrations every 400–500 μm across the cortical surface to examine the neuronal activities across the region of the hand and face representations in area 3b (Sur et al., 1982). Parts of areas 3a and 1 were also mapped for the purpose of defining rostral and caudal boundaries of area 3b. The receptive fields for multiunit recording sites were determined by lightly touching the skin with fine probes, brushing the hairy skin, tapping muscles, and moving joints (Qi et al., 2011a). Neurons in area 3b have small, discrete receptive fields and are sensitive to low threshold, cutaneous stimulation. Area 3a neurons are distinguished by a tendency to respond to tapping and muscle or joint manipulations. Area 1 neurons respond to touch, but generally have larger receptive fields, and the area has a different somatotopy that mirrors that of area 3b. The physiological borders of area 3b and adjacent areas 3a and 1 were identified and marked by electrolytic lesions in some instances.

Perfusion and Histology

Two weeks after the tracer injections in the cuneate nucleus, monkeys were euthanized with a lethal dose of sodium pentobarbital (120 mg/kg). Perfusion was initiated through the ascending aorta with phosphate buffered saline (pH 7.4) and continued with 2% or 4% paraformaldehyde in phosphate buffer and 10% sucrose containing fixative. The brainstem and spinal cord were removed and stored in the phosphate buffer containing 30% sucrose overnight for cryoprotection. We identified the cervical segments according to the rostrocaudal borders of dorsal roots and marked certain segments by placement of pins dorsoventrally through the spinal cord. The cervical spinal cord was then dissected from the remaining tissue. This strategy allowed us to identify the levels of cervical segments after the tissue was cut. Both the brainstem and cervical spinal cord were cut in the transverse plane at a thickness of 50 μm on a freezing microtome, the rest of spinal cord including thoracic, lumbar and sacral segments were cut in the horizontal plane. For different histological purposes, sections of the brainstem were divided into 4 or 5 series (B-HRP/cytochrome oxidase (CO)/CTB/VGLUT2/BDA or FR). Sections of the cervical spinal cord were divided into 5 or 6 series (CO/FR or BDA/CTB1/Nissl or NeuN/CTB2/saved), and of the thoracic, lumbar and sacral spinal cord were divided in 3 or 4 series (CO/BDA or FR/CTB).

Sections with expected fluorescent label were directly mounted without further staining procedure, air-dried, coverslipped, and kept in the dark at 4°C. One series of the brainstem and spinal cord sections was processed with a standard method of 3,3,5,5-Tetramethylbenzidine reaction (TMB; Gibson et al., 1984) to reveal the central projections from the skin of digits 1, 3 and 5 of both hands. Two more series were separately processed to reveal the CTB (1:4,000 dilution, goat anti-CTB; List Biological Labs) or BDA (PK-6100; Vector Laboratories, Burlingame, CA) label in the brainstem and spinal cord (see details in Liao et al., 2013). One series of spinal cord sections was processed for NeuN (1:

5000 dilution, monoclonal mouse anti-NeuN; Millipore, Billerica, MA) or Nissl staining to reveal the laminar organization (Fig. 1; see Sengul et al., 2013). Cytochrome oxidase (CO) or vesicular glutamate transporter 2 (VGLUT2; monoclonal mouse-anti-VGLUT2; Millipore) staining was used to reveal the brainstem architecture (Qi et al., 2011b; Wong-Riley, 1979).

Antibody characterization

We used NeuN and VGLUT2 antibodies in the present study (NeuN: AB_2298772; VGLUT2: AB_262186; Table 1). Monoclonal anti-NeuN (MAB377) from Millipore is a mouse IgG1 antibody with clone A60. It was prepared against purified cell nuclei from mouse brain, and specifically recognize the DNA-binding, neuron-specific protein NeuN in most CNS and PNS neuronal cells in vertebrates including primates (Balaram and Kaas, 2014; Rovo et al., 2012). This antibody labels 2–3 bands in the 46–48kDa range and possibly another band at approximately 66kDa in western blot preparation (adapted from product information). Another antibody, monoclonal anti-VGLUT2 (MAB5504) is a mouse IgG1 antibody with clone 8G9.2, which was developed against recombinant protein from rat VGLUT2, and labels a single band at 56kDa (Balaram et al., 2013). Immunoreactivity of anti-VGLUT2 accurately recognizes VGLUT2 in primates (Balaram et al., 2013; Balaram and Kaas, 2014; Baldwin et al., 2013) and rats (Kaneko and Fujiyama, 2002).

Data analysis

We analyzed the distributions of labeled neurons in sections of cervical segments of the spinal cord after tracers were injected into the cuneate nucleus in normal and dorsal column lesioned cases. We focused on the distribution of neurons labeled in spinal laminae III–IV, where neurons receive inputs from cutaneous afferents (Willis and Coggeshall, 1991). An upright microscope (Nikon E800 microscope) was used to locate the injection sites in the brainstem and labeled profiles in the spinal cord. Images were digitally captured by a Nikon DXM 1200 camera, which was mounted on the microscope. We exported the images to Adobe Photoshop CS6 (Adobe Systems, San Jose, CA) for adjustments of brightness and contrast.

Evaluating the extents of dorsal column lesions—Three methods were used to evaluate the completeness of dorsal column lesions. First, the visible extent of the lesion was reconstructed from transverse sections of the spinal cord. Second, the neuronal responsiveness in the deafferented hand representation of area 3b contralateral to the lesion site was examined two weeks after lesion. Third, B-HRP injections into matching locations of both hands labeled spared afferents in the deprived cuneate nucleus in comparison with those labeled in the non-deprived cuneate nucleus (SqM 13-01). This procedure did not provide useful data in cases SqM 12–52 and SqM 13–17 because the tracer leaked out during injections. Here, we used the percentage of B-HRP labeled regions in the cuneate nucleus of the lesioned side to those of the control side as a quantitative measure of the completeness of lesion (see Qi et al., 2011a). In brief, we captured images of the B-HRP labeled foci in the brainstem with darkfield microcopy. Digital images were converted into 8-bit grayscale images using ImageJ Software (National Institutions of Health, Bethesda, MD). The threshold was adjusted to appropriately select the B-HRP labeled foci across

rostrocaudal sections. The total number of selected pixels, which was later converted into square millimeters, represents the areal sum of the labeled foci across individual locations. The areas of the B-HRP-labeled regions in the brainstem of the non-lesioned side and lesioned side were statistically compared using a *t*-test (SigmaPlot 11.0, San Jose, CA). Statistical significance was considered for $p < 0.05$. The percentage of the completeness of dorsal column lesion was expressed as: 100 × the total labeled area on the lesioned side/total labeled area on the control side.

Locations of labeled spinal neurons and axons in the cervical segments—The locations of CTB-, BDA- and FR-labeled neurons in the cervical spinal cord were plotted using the Neurolucida system (MBF Bioscience, Williston, VT). In cases with BDA or FR injections, labeled fibers in the spinal cord were identified and plotted. Special care was taken to mark blood vessels and landmarks for the alignment of plots of labeled cells to adjacent NeuN or Nissl sections in the Adobe Illustrator CS6 (Adobe Systems). This allowed us to quantify the numbers of labeled neurons in each laminae of individual sections. Since certain segments of the cervical spinal cord were marked by the placements of pins, we were able to categorize spinal cord sections into C1 to C8 segments accordingly. The percentage of labeled neurons in individual laminae of one cervical segment across the cervical spinal cord ipsilateral to the injection in each monkey was calculated by: 100 × the number of labeled neurons in the lamina of a particular segment/the number of total labeled cells in cervical spinal cord. The data were used to generate heat maps of the distributions of labeled neurons in the cervical spinal cord (common log with range 0.1 to 10; SigmaPlot). We calculated the percentage of labeled neurons in individual laminae in each cervical segments in every monkey by: 100 × the number of labeled neurons in the lamina of a particular segment/the number of total labeled cells in this segment.

The impact of the dorsal column lesion on the percentage of spinal cord neurons with control projections to the cuneate nucleus was estimated by comparing numbers of labeled neurons in segments C1 to C3, which are above the lesion level, to numbers of labeled neurons in segments C4 to C8, which are below the lesion, with a *t*-test. In order to see if the dorsal column lesion alters the laminar origins of spinal cord neurons that projected to the cuneate nucleus, we separately calculated percentages of labeled neurons in individual laminae from C1–C3 (or C4–C8) by: 100 × the number of labeled neurons in the lamina from C1–C3 (or C4–C8)/the number of total labeled cells in C1–C3 (or C4–C8). We also compared the configurations of laminar distribution of the labeled neurons in segments C1 to C3 and in segments C4 to C8 between these two groups by Two Way Anova with the *post hoc* Student-Newman-Keul Method. Statistical significance was considered for $p < 0.05$. Data are reported as mean ± standard error of the mean (SEM).

RESULTS

The results indicate that in normal monkeys large numbers of neurons in the cervical spinal cord project to the cuneate nucleus, and that many of these neurons, but not all, project via axons that join the cuneate fasciculus. Others survive lesions of the dorsal column at the C4 level by ascending in the lateral funiculus, and may contribute to the reactivation of somatosensory cortex. Here we first describe the laminar distribution of spinal cord neurons

that are labeled after injections of tracers into the cuneate nucleus, then the spinal pathways of these neurons to the cuneate nucleus, and finally the locations of spinal cord neurons that are labeled by cuneate nucleus injections after dorsal column lesion at the C4 level. Microelectrode recordings from somatosensory cortex were used as one measure of the effectiveness of the spinal cord lesions.

The locations of spinal cord neurons that project to the cuneate nucleus

Each CTB injection into the cuneate nucleus of three different monkeys labeled large numbers of neurons in the dorsal horn laminae of the ipsilateral cervical spinal cord. Slight variations in the locations and extents of the injection cores were reflected in the numbers and distributions of labeled neurons. Results from the three cases are considered separately.

In owl monkey 11–18, CTB was injected into the cuneate nucleus of the left side and the gracile nucleus of the right side (Fig. 2A). Labeled neurons on the left side were almost exclusively in the cervical spinal cord. As few neurons were labeled in the contralateral side after a single cuneate nucleus injection in other cases (see Figs. 3 and 4), almost all the labeled neurons on the left side reflect the CTB injection on the left side. This injection on the left side included the part of the cuneate fasciculus and extended into the cuneate nucleus. Examples of distributions of labeled neurons at the C3 and C6 levels in the dorsal horn of the spinal cord are shown in Figure 2B and C. A more complete distribution of labeled neurons is illustrated for spinal cord sections at levels C1–C8. Finally, the percentage of labeled neurons throughout spinal cord lamina I–X (Rexed, 1952) for each cervical segment 1–8 is indicated relative to the total across segments (red) or the total within that segment (blue). Even though the injection directly involved only part of the left cuneate nucleus, 2917 CTB-labeled neurons were found on the left side of the cervical spinal cord and a few additional neurons were labeled in the thoracic spinal cord. Since inputs from second-order neurons in cervical spinal cord likely relay inputs from the hand to the deprived cuneate nucleus, we restricted our analysis to the labeled neurons in C1–C8 segments. Most of the labeled neurons within the dorsal horn of the spinal cord were found in lamina IV, as compared to the total labeled neurons within that segment (Fig. 2E blue) or across all C1–C8 segments (Fig. 2E red). Overall, 70% of labeled neurons were in lamina IV, 14% in lamina V–VI, 10% in lamina III, and 6% in other layers. Some neurons might have been labeled as result of damaged axons in the cuneate fasciculus taking up the CTB (Chen and Aston-Jones, 1995).

The other injection in the same case was largely confined to part of the gracile nucleus representing the hindlimb and adjoining trunk. A small part of the cuneate nucleus appeared to be included (Fig. 2A). As a result, most of the labeled neurons from this injection were in the ipsilateral thoracic and lumbar spinal cord, with a few neurons in the contralateral thoracic spinal cord (not shown). As shown in Figure 2D, a few labeled neurons were scattered in the right cervical spinal cord, mainly in laminae III and IV. These labeled neurons could reflect a slight involvement of the injection core, or even the uptake of CTB by damaged axons of passage in the cuneate fasciculus (Chen and Aston-Jones, 1995)

Similar results were obtained in two control squirrel monkey cases with single unilateral injections of CTB into the left cuneate nucleus. In squirrel monkey 11–30, the CTB injection

targeted zone in the left cuneate nucleus where neurons responded to light touches on digits 3 and 4 of the left hand. The injection core extended approximately 800 μm rostrocaudally, covering much of the depth of the cuneate nucleus and the overlying cuneate fasciculus, and the most lateral region of gracile nucleus (Fig. 3A). The injection labeled 1012 neurons in the ipsilateral cervical spinal cord and 13 neurons in the contralateral cervical spinal cord (Fig. 3). Labeled neurons were distributed across all segments of the ipsilateral cervical spinal cord, and were primarily concentrated in dorsal horn laminae III (27%) and IV (71%). Only a few labeled neurons were in other laminae (2%). In addition, 255 labeled neurons were in the ipsilateral thoracic spinal cord, and 22 were in the ipsilateral lumbar spinal cord, perhaps reflecting the slight spread of tracer injection site into the gracile nucleus. On the contralateral side, 62 labeled neurons were in the thoracic spinal cord, whereas only 1 neuron was identified in the lumbar spinal cord. Note that the numbers of labeled neurons in the cervical and thoracic plus lumbar spinal cord are not fully comparable because of the different cutting planes of the sections (transverse or horizontal). In squirrel monkey 12-04, an injection of CTB was placed in a part of the left cuneate nucleus that responded to touch on digits 3 and 4 and palmar pads 1 and 2. The injection core extended about 1 mm rostrocaudally, and included much of the depth of the cuneate nucleus and some of the adjoining cuneate fasciculus (Fig. 4A). The injection labeled 675 neurons in the ipsilateral cervical spinal cord and a few in the contralateral cervical spinal cord (Fig. 4D). Labeled neurons were distributed across all cervical spinal cord segments, and were concentrated in laminae III (23%) and IV (67%), with fewer in laminae V and VI (8%) and other laminae (2%). Small numbers of labeled neurons were present in the thoracic (n = 17) and lumbar (n = 7) segments ipsilateral to the injection site. Only 2 labeled neurons were found in the contralateral thoracic spinal cord.

Overall, the results across the three cases indicate that large numbers of spinal cord neurons project to the cuneate nucleus. In addition, the vast majority of these neurons are distributed across laminae III and IV of segments 1–8 of the ipsilateral cervical spinal cord.

Axon pathways connect the ipsilateral cuneate nucleus with the cervical dorsal horn through the cuneate fasciculus and the lateral funiculus

We studied the courses of the axons that travel between the cervical spinal cord and the cuneate nucleus in two control squirrel monkeys. Our strategy involved injecting bidirectional tracers into the hand representation of the cuneate nucleus and then examining the distribution of fibers labeled within the spinal cord. In squirrel monkey 11–30, we placed a focal injection of FR in the right cuneate nucleus where we recorded multiunit responses to light touch on digits 1–3 and the adjoining palm. The injection core was restricted to the cuneate nucleus (Fig. 5A). The injection labeled both spinal cord neurons and axons. As in other cases, the labeled neurons were almost exclusively in the ipsilateral cervical spinal cord (Fig. 5D). Labeled axons in the cuneate fasciculus and lateral funiculus were found above C5 levels (Fig. 5B–D). More labeled axons were in the cuneate fasciculus pathway. Similar results were obtained after an injection of BDA into the part of the right cuneate nucleus representing digits 1–3 and the adjoining palm of right hand in squirrel monkey 12-04 (Fig. 6). The injection core was restricted to the cuneate nucleus, although the uptake zone may have spread slightly beyond the ventral border (Fig. 6A). Typically, the BDA

injections do not effectively retrogradely label neurons (Vercelli et al., 2000), although a few neurons were labeled in lamina IV of the ipsilateral dorsal horn of the cervical spinal cord in this case. In addition, axon terminations in the dorsal horn were also labeled. These results indicate that both the cuneate fasciculus and the lateral funiculus carry axons that connect the neurons in the cuneate nucleus with neurons in the ipsilateral cervical dorsal horn of the spinal cord. As both injections labeled cell bodies in the dorsal horn, and both injected tracers likely label axon of neurons in the cuneate nucleus, the labeled axons could reflect projections from the cuneate nucleus to the cervical spinal cord, as previously revealed in monkeys (Burton and Loewy, 1977), or axons of spinal cord neurons projecting to the cuneate nucleus (Rustioni, 1977; Rustioni et al., 1979), or, most likely, both.

Spinal projections to the cuneate nucleus after dorsal column lesions

Having established the organization of the spinocuneate connections in control monkeys, we then asked if those projections to the cuneate nucleus remained after a high cervical dorsal column lesion. In order to completely remove the direct afferents from the hand, we sectioned the dorsal column in three squirrel monkeys. The lesion was made at the C4 level of the spinal cord, which is where inputs from digits 1 to 5 and palm enter the spinal cord through segments 4 to 7 (Florence et al., 1991). This procedure removes the major activating inputs to the ipsilateral cuneate nucleus. Consequently the contralateral ventroposterior nucleus (VP) and area 3b of primary somatosensory cortex are deprived of most of their activating inputs (Fig. 7) and are unresponsive to tactile stimuli for weeks to months (Kaas et al., 2008; Qi et al., 2011a). The extents of the lesions in the spinal cord were determined histologically, and the neuronal responsiveness in the contralateral area 3b was determined to further evaluate the effectiveness of the dorsal column lesions (see Materials and Methods). The effectiveness of dorsal column lesion was additionally revealed by the reduction of B-HRP labeling in the deprived cuneate nucleus after B-HRP was injected into two hands in case 13-01. Results from these three monkeys are described below.

The dorsal column lesion in squirrel monkey 12–52 was extensive, involving the entire right cuneate fasciculus, dorsal horn on the right side, and ventral portions of dorsal columns on the both sides (Fig. 7). Two weeks after lesion, we mapped the expected representations of hand and face in area 3b of the contralateral parietal cortex (Fig. 7). Light touch and taps on the hand did not evoke neuronal responses in the deprived hand representation. However, light touches of the face evoked robust neuronal responses in the face representation, indicating that the inactivation of the hand representation resulted from the dorsal column lesion instead of anesthetic depression.

Both examinations of the lesion site and of cortical responsiveness in the contralateral somatosensory cortex indicated that the dorsal column lesion interrupted all traveling fibers in the right cuneate fasciculus. A focal injection of CTB in the representations of digits 2 to 4 of the right cuneate nucleus was immediately followed by the dorsal column lesion at the C4 level (Fig. 8A). The injection core rostrocaudally extending about 800 μm was almost completely restricted to the cuneate nucleus with slight spreading beyond the ventral border. The lesion greatly altered the distribution and reduced the number of spinal cord neurons projecting to the cuneate nucleus. The injection labeled 460 neurons in the ipsilateral

cervical spinal cord. The majority of CTB-labeled neurons (n = 409) were found above the level of the dorsal column lesion in the high cervical levels C1–C3 (Fig. 8B, D). These CTB-labeled neurons were largely in the laminae IV (71%) and V–VI (21%), with fewer in lamina VII (4%) and other layers (3%; Fig. 8E). The numbers of CTB-labeled neurons below the dorsal column lesion were significantly reduced (P = 0.005, t-test). However, we were able to identify 51 labeled neurons from C4 to C8. One representative example of the labeled neurons in the C5 is shown in Figure 8C. The majority of the labeled neurons from C4–C8 were still located in the lamina IV (43%), with fewer of them in laminae V–VI (18%) and III (12%). Some labeled neurons were noted in spinal laminae VII (10%) and VIII (10%), and even smaller numbers were present in laminae II (4%) and X (3%). In the contralateral side, we identified 25 CTB-labeled neurons in total. These labeled neurons were mainly noted in segments C1 to C3 (n = 19). Thirteen labeled neurons were in the lamina IV, 4 of them were located in laminae V–VI. Two labeled neurons were noted in laminae III and VIII. Only 6 labeled neurons were identified in C4–C8. Three of them were in the laminae V–VI, 2 were in the lamina VII and only one labeled neuron was present in the lamina IV. We also identified labeled neurons in the ipsilateral thoracic (n = 2) and lumbar (n = 1) spinal cord, and a total of 3 neurons (2 in thoracic and 1 in lumbar) on the contralateral side. The results indicate that the C4 dorsal column lesion removed the majority of the second-order spinal cord projections to the cuneate nucleus. Yet a small number of neurons, roughly 12%, with such projections remained below the lesion level.

Similar results were obtained in the second case. In squirrel monkey 13–17, the lesion was at the spinal C4 level involving most of the right dorsal columns, the medioventral region of the left dorsal columns, medial regions of the dorsal horn on both sides, and the central canal region (Fig. 9A). The dorsolateral corner of the right cuneate fasciculus, which is close to the dorsal root entry zone, was spared. Two weeks after the spinal cord lesion, we mapped the contralateral (left) parietal cortex to validate the extent of dorsal column lesion (Fig. 9B). Ninety-five penetrations were made in the expected hand representation. Neurons in three penetrations responded weakly to the cutaneous stimulation on the hairy radial hand and one penetration responded to stimulation on the dorsal, hairy digit 1. Eight out of the 11 penetrations in the face representation were highly responsive to lightly touching and brushing the chin. Two at the hand-face border and 1 in area 3a were weakly responsive. Accordingly, the dorsal column lesion likely interrupted most inputs from the forelimb, but spared few afferents from the dorsal hand. The CTB injection in this case was in the representations of digits 2–4 in the right cuneate nucleus and confined to the cuneate nucleus and cuneate fasciculus (Fig. 10A). Appropriately 1000 μm of rostrocaudal spread of the injection core was observed. A total of 676 CTB-labeled spinal cord neurons, 648 on the ipsilateral side and 28 in the contralateral side, resulted from the injection. The majority of CTB-labeled neurons (587/648) were found in the ipsilateral cervical segments C1 to C3, which significantly outnumbered the labeled neurons in individual cervical segments below the lesion (61/648; p = 0.002; Fig. 10D). The different densities of labeled neurons in the spinal cord above and below the lesion are shown in representative sections from C3 and C6 segments (Fig. 10B and C). Above the lesion, the laminar analysis revealed that CTB-labeled neurons were mostly distributed in laminae IV (78%) and V–VI (15%), and slightly fewer neurons were in the lamina VII (3%) and III (2%). Eight CTB-labeled neurons were

scattered in spinal laminae I and VIII. The laminar distribution of labeled neurons below the lesion was in a somewhat similar pattern with 48% of the labeled neurons found in the lamina IV, 20% in lamina III and 18% in laminae V–VI. Few labeled neurons were noted in laminae I, VII and XI. In the contralateral cervical spinal cord, 22 labeled neurons were found in the higher cervical spinal cord C1 to C3 in the laminae VII (50%), IV (23%), V–VI (18%), III (5%) and VIII (4%). Only 6 labeled neurons in the contralateral dorsal horn were scattered from C4 to C8. Thus, roughly 9% of the preserved spinal cord inputs to the cuneate nucleus were from second-order spinal cord neurons below the lesion. We found these labeled neurons on each side of the thoracic spinal cord ($n = 6$) and two labeled neurons in the contralateral lumbar spinal cord.

In our third case, squirrel monkey 13-01, the sparring of axons in the dorsal column was greatest. In this monkey, the dorsal column lesion was at the C4 level and restricted to the area between the posterior median sulcus and the posterior intermediate sulcus to the bottom of the dorsal columns, which mainly involved the cuneate fasciculus (Fig. 11A). The dorsolateral region of the cuneate fasciculus close to the dorsal root entry was avoided. The subcutaneous B-HRP injections in the digits 1, 3 and 5 of both hands resulted in dense patches in the dorsal horn on the two sides at C5, C6 and C7 levels. However, the B-HRP labeling in the cuneate nucleus on the lesioned and control sides was in a different pattern. Patches of B-HRP labeling were easily noted in the cuneate nucleus on the left side, while only a few small foci of B-HRP labeled terminals were noted in the corresponding locations in the right cuneate nucleus (Fig. 11B arrowheads). The combined areas of B-HRP labeled foci in the left cuneate nucleus (0.11 mm^2) were significantly larger than the combined areas of the labeled foci in the right cuneate nucleus (0.01 mm^2; $p < 0.001$, *t*-test; Fig. 11B), producing an estimated 91% completeness of the dorsal column lesion in this case. We also mapped the representations of hand and face in the area 3b contralateral to the spinal cord lesion side (Fig. 12). Receptive fields identified from 122 penetrations in the lateral parietal cortex revealed a somatotopic progression of hand representation that was very similar to that found in normal squirrel monkeys (Sur et al., 1982). Thus, the representations of digits 1 to 5 were arranged in a mediolateral sequence, the distal digits pointed rostrally and the palm representation was located caudally (Fig. 12B). Recording from the adjoining rostral area 3a and the caudal area 1 revealed reversed somatotopies. However, most of neurons recorded in the penetrations in the hand representation had weak, or very weak responses, and more of them were responsive to the dorsal, hairy hand than in normal monkeys. These observations suggested that the dorsal column lesion spared some afferents originating from digits 1–5 and palm, but most of the inputs were lost. This interpretation is consistent with the anatomical evidence that peripheral inputs from digits 1, 3 and 5 of the right hand were reduced by an estimated 91%.

CTB was injected into the representations of digits 2 and 3 of the right cuneate nucleus (Fig. 13). The injection core involved the cuneate nucleus and fasciculus, with a slight spread beyond the ventral border (Fig. 13A). We identified a total of 1030 CTB-labeled neurons in the ipsilateral cervical spinal cord. Although the numbers of the labeled neurons in the individual segments (C4–C8) below the lesion were significantly reduced from the numbers of labeled neurons in C1 to C3 above the lesion ($n = 951$; $p < 0.001$), 79 labeled neurons

were present in segments C4–C8. The labeled neurons above the lesion were mostly located in the lamina IV (67%), with a decreased projection in laminae V–IV (19%), and even fewer numbers in the lamina III (7%). Few labeled neurons were present in other laminae (7%). The labeled neurons below the lesion were distributed in a slightly different pattern. The majority of labeled neurons were in laminae V (39%) and IV (34%), while 14% and 9% of labeled neurons were in laminae VII and III. Few labeled neurons were scattered in laminae VIII–X. In the cervical spinal cord contralateral to the cuneate nucleus injection, 34 labeled neurons were identified from C1 to C3 and 15 neurons were found from C4 to C8. Most of the labeled neurons were distributed in the lamina IV (37%), and to lesser numbers in laminae V–IV (29%), VII (18%) and III (12%). Only 2 labeled neurons were identified in the lamina IX. Thus, with the sparring of perhaps 9% of the primary sensory axons in the cuneate fasciculus, the C4 lesion produced a residual of roughly 8% of the projections from spinal cord neurons below the lesion to the cuneate nucleus. No labeled neurons were identified in thoracic, lumbar and sacral spinal cord in this case.

Comparison of locations of spinocuneate neurons in control and dorsal column lesioned animals

The distributions of CTB-labeled ipsilateral spinal cord projections to the cuneate nucleus for the 6 cases are summarized the Figure 14. The results are represented by the percentages of labeled neurons in individual laminae of C1–C8 in each case. It is apparent that spinal cord neurons that projected to the ipsilateral cuneate nucleus were primarily distributed in the laminae IV throughout the cervical spinal cord in normal monkeys (Fig. 14A). The labeled neurons in the three dorsal column lesioned monkeys were concentrated above the level of lesion, mainly in the laminae IV. Nevertheless, a small number of labeled neurons remained below the lesion in C4–C8. We compared the laminar distributions of the labeled neurons in individual segments that are above and below the lesion site. The spinal cord neurons that projected to the ipsilateral cuneate nucleus above the lesion (Fig. 14B) were a similar laminar distribution in both normal and dorsal column lesioned monkeys ($p = 0.309$). However, the short-term dorsal column lesion (2 weeks) significantly altered the laminar organization of remaining neurons that were labeled below the lesion ($p < 0.001$; Fig. 14C). Although the origins of spinocuneate projections were still mainly from spinal lamina IV, the ratios of cuneate nucleus inputs from laminae V–VI and VII were significantly increased. Thus, the numbers of labeled neurons below the lesion level were notably reduced after dorsal column lesions and more of them were in laminae V–VI.

The ratio of the total number of labeled neurons in C1–C3 to the total number of labeled neurons in C4–C8 obtained from the three normal cases reveals the typical distribution of second-order spinal cord neurons in the cervical spinal cord. Overall, the CTB injections in the cuneate nucleus in these three cases labeled a total of 4604 neurons in the cervical spinal cord ipsilateral to the injections. Among which, 1611 labeled neurons (35%) were in C1–C3 levels and 2993 labeled neurons (65%) were in C4–C8 levels, producing a ratio of 1.85 of the spinal cord neurons in C4–C8 levels when compared to those in C1– C3 levels. In the three cases that received complete or nearly complete dorsal column lesions at the C4 level, a total of 2138 labeled neurons were identified after the CTB injections. The majority of labeled neurons ($n = 1949$, 91%) were distributed above the lesion, whereas a small number

of labeled neurons (n = 191, 9%) were identified below the lesion. According to the expected ratio of 1.85 obtained from the normal cases, the expected number of labeled neurons in C4–C8 levels of the three dorsal column lesioned cases is 3601. However, we were able to identify only 191 labeled neurons. The results suggested that roughly 5.3% of inputs from the spinal cord neurons below the lesion continue to project to the cuneate nucleus after the lesions of cuneate fasciculus pathway, albeit the small number of neurons stands for 9% of the total inputs from the cervical spinal cord neurons after the lesion.

Finally, the results also indicate that a small number of neurons in the spinal cord project to the contralateral cuneate nucleus. These neurons, as for their much larger numbers in the ipsilateral spinal cord, were mainly in lamina IV. As the cuneate nucleus represents inputs from the ipsilateral body, it is not known how these inputs from the contralateral spinal cord influence processing in the cuneate nucleus.

Discussion

After complete or nearly complete lesions of the dorsal columns at a high cervical level in monkeys, the contralateral hand representation in primary somatosensory cortex (area 3b) becomes unresponsive to tactile stimuli. However, over postlesion weeks, this cortex recovers responsiveness to touch on the hand (Qi et al., 2014b). Our present study is part of a more extensive effort to determine the sources of this functionally important reactivation. First, we confirm that a complete lesion of the cuneate fasciculus at the C4 level completely deactivates the contralateral hand representation in area 3b for at least 2 weeks. Second, we add to previous evidence for reactivation in a nearly normal somatotopic pattern after large dorsal column lesions (Jain et al., 1997; Qi et al., 2011a) by showing that a nearly normal representation of touch can be present in area 3b as early as two weeks after a cuneate fasciculus lesion estimated to be 91% complete. Third, consistent with previous reports in other species, we determined that large numbers of cervical spinal cord neurons project to the cuneate nucleus, providing a potential source of reactivation of area 3b. Fourth, consistent with limited evidence from other species, many or most of the spinal cord neurons join the cuneate fasciculus or the dorsolateral axon pathway. Thus, cutting the cuneate fasciculus at a high cervical level eliminates most, but not all, of the second-order spinal cord projections to the cuneate nucleus. Fifth, we show that cutting the cuneate fasciculus at the C4 level does remove roughly 95% of the projections to the cuneate nucleus from neurons below the lesion.

The representation of somatosensory cortex after lesions of the dorsal column

Our results indicate that a complete lesion of the cuneate fasciculus at the C4 level renders the hand representation in contralateral somatosensory cortex (area 3b) unresponsive to tactile stimuli for two weeks or more. However, if even a few axons survive (e.g., 1%), these axons may weakly activate small islands of neurons within the landscape of deactivated neurons in the hand representation after two weeks of recovery. Moreover, with approximately 10% preserved cuneate fasciculus primary axons, a somewhat weak but nearly normal somatotopic hand representation can be present after two weeks. Previously, it was known that the hand cortex is immediately deactivated after large lesions of the dorsal

column, although small islands of hand cortex may respond after incomplete lesions within days of recovery. A highly normal somatotopy may appear after weeks or months of recovery, and abnormal somatotopies may appear after recoveries of 6–8 months or more, including activation of hand cortex by touch on the face or arm. Most of these previous findings were from studies on New World squirrel, owl, or marmoset monkeys whose hand cortex is on the surface of cortex and more easily mapped with microelectrodes (Bowes et al., 2013; Bowes et al., 2012; Chen et al., 2012; Jain et al., 1997; Jain et al., 2000; Qi et al., 2011a). More limited but similar results have been obtained from macaque monkeys (Jain et al., 2008). Much of the cortical reactivation and somatotopy likely depends on the formation of new activating connections and synapses in the cuneate nucleus (Kaas et al., 2008; Qi et al., 2014a), as reactivations after sensory loss occur in the cuneate nucleus (Xu and Wall, 1997, 1999) and thalamus (Jain et al., 2008; Weng et al., 2003), and in higher areas of somatosensory cortex (Bowes et al., 2013; Bowes et al., 2012; Tandon et al., 2009; Wang et al., 2013). Clearly preserved dorsal column afferents can play an important role in the reactivation process, and treatments that promote axon spouting and the formation of new connections in the cuneate nucleus can enhance the reactivation of cortex by these preserved afferents (Bowes et al., 2012). However, extensive reactivations occur when all or nearly all of these first order inputs to the cuneate nucleus are removed (Qi et al., 2011a).

Large numbers of neurons in the cervical spinal cord project to the cuneate nucleus

Our injections of retrograde tracers into the cuneate nucleus of squirrel monkeys consistently labeled large numbers of neurons in the cervical spinal cord. While our injections were confined to only part of the cuneate nucleus, up to 1012 spinal cord neurons were labeled. These neurons were mainly in ipsilateral dorsal horn laminae, with a few in contralateral laminae. They included cervical segments 1–8, with an occasional neuron in upper thoracic segments. Importantly, most of the labeled neurons were in laminae III and IV, which are known to receive inputs from low threshold cutaneous afferents (Price and Mayer, 1974; Schneider, 2008; Wagman and Price, 1969).

In addition, our tracing studies indicate that axons that connect the cervical spinal cord with the cuneate nucleus travel in the cuneate fasciculus and the dorsolateral funiculus. However, some or all of the labeled axons in these two pathways could have been descending projections from the cuneate nucleus (Burton and Loewy, 1977). Spinal cord neurons projecting to the dorsal column nuclei have been described for rats (de Pommery et al., 1984; Giesler et al., 1984) and cats (Enevoldson and Gordon, 1989a; Rustioni and Kaufman, 1977). Previous observations in primates were limited. Rustioni (1977; 1979) injected HRP as a retrograde tracer into dorsal column nuclei of macaque monkeys and found labeled neurons mainly in lamina IV of the ipsilateral dorsal horn, but also scattered in other laminae and few in the contralateral dorsal horn. As injections likely included the gracile nucleus, labeled neurons were found in the lumbar as well as the cervical spinal cord. Labeled spinal cord neurons were found to have axons that ascended in the dorsal columns and the dorsal part of the lateral funiculus, suggesting that our injections in the cuneate nucleus labeled ascending projections. Cliffer and Willis (1994) also revealed projections from the dorsal horn of the cervical spinal cord to the cuneate nucleus of macaque monkeys via the dorsal columns, but they did not detect labeled axons in the dorsolateral funiculus.

Section of the cuneate fasciculus greatly reduced projections of cervical spinal cord neurons to the cuneate nucleus

Perhaps the most important contribution of our present study was that complete or nearly complete lesions of the cuneate fasciculus at the C4 level reduced the numbers of labeled neurons in the cervical spinal cord below the lesion by roughly 95%, while producing no notable reduction in such neurons at cervical levels above the lesion. This indicates that most of the projecting neurons below the C4 have axons that enter the dorsal column below the lesions, while only a small number avoid the lesions by traveling in the dorsolateral funiculus or by joining the dorsal columns above the lesions. Thus, only a small number of cervical spinal cord neurons below the C4 are available to contribute to the reactivation of somatosensory cortex two weeks after a complete lesion of the cuneate fasciculus. Possibly with longer recovery times, some damaged axons could sprout and reach the cuneate nucleus, but this is yet unknown. The role of spinal cord neurons above the level of the lesions that continue to project to the cuneate nucleus is also unknown, but primary axon inputs from the hand enter the spinal cord below C4 (Florence et al., 1988, 1991). Another uncertainty concerns the response properties of the spinal cord neurons that project to the cuneate nucleus, as these properties are not well established. To contribute to cortical reactivation, they would be expected to have small receptive fields and respond to light tactile stimulation (Qi et al., 2014b). While earlier studies of second-order neurons in the dorsal horn of rats and cats focused on responses to both tactile and noxious stimuli (Bennett et al., 1984; Giesler and Cliffer, 1985), most second-order neurons projecting to the cuneate nucleus are in or near lamina IV, which has appropriate tactile peripheral axon inputs in mammals (Willis and Coggeshall, 1991). While little is known about the functional properties of spinal cord neurons projecting to cuneate nucleus in monkeys, a recent study in raccoons, a carnivore with highly sensitive glabrous forepaws somewhat like monkeys, revealed that much laminae III and IV neurons respond to light tactile stimulation, and have small receptive fields often restricted to a single digit pad (Dick et al., 2001), properties very much like those from primary afferents from the glabrous forepaw. Because second-order neurons activate cuneate nucleus with a slightly longer delay, they are usually considered to be modulatory rather than driving (e.g. Dick et al., 2001). This conclusion is consistent with the lack of cortical responsiveness to tactile stimulation for as long as two weeks or more after section of the cuneate fasciculus. However, the reactivation of cortex over longer recovery times, previously attributed to the strengthening of synaptic inputs from surviving primary cutaneous inputs (Kaas et al., 2008; Qi et al., 2014a), could be complimented by spinal cord neuron inputs that are strengthened from being modulatory to becoming driving due to reduced synaptic competition, axon growth, and synapse formation over weeks of recovery time.

Another possibility is that some damaged or cut projections to the cuneate nucleus from spinal cord neurons recover or regenerate over longer survival times to contribute to the reactivation of the cuneate nucleus and contralateral somatosensory cortex. This possibility and the possible roles of pathways that bypass the cuneate nucleus are under investigation.

Conclusion

In this study, we provide evidence for a possible role for second-order spinal cord neurons in cortical reactivation. We found that approximately 5% of projections from second-order neurons in the cervical spinal cord below the C4 dorsal column lesion continued to ascend to the ipsilateral cuneate nucleus by travelling in the lateral funiculus. These surviving neurons were mainly in lamina IV of the dorsal horn in spinal cord, which conveys tactile information from periphery to the somatosensory system. Given that much of the deactivated somatosensory cortex becomes responsive to touch over weeks to months of recovery after complete or nearly complete dorsal column lesions, we propose that the second-order spinal cord pathway contributes to the cortical reactivation after spinal cord injury, probably by synaptogenesis and sprouting in the cuneate nucleus over longer recovery times.

Acknowledgments

Funding: This study is supported by NIH grant NS16446 to J.H.K., NIH grant NS067017 to H.X.Q., NIH grant K99 NS079471 to O.A.G.

We are grateful to Charnese Bowes for assistance in data collection, Laura Trice for help with histological procedures and Mary Feurtado for surgical assistance.

Literature Cited

Balaram P, Hackett TA, Kaas JH. Differential expression of vesicular glutamate transporters 1 and 2 may identify distinct modes of glutamatergic transmission in the macaque visual system. J Chem Neuroanat. 2013; 50–51:21–38. [PubMed: 19594444]

Balaram P, Kaas JH. Towards a unified scheme of cortical lamination for primary visual cortex across primates: insights from NeuN and VGLUT2 immunoreactivity. Front Neuroanat. 2014; 8:81. [PubMed: 25177277]

Baldwin MK, Balaram P, Kaas JH. Projections of the superior colliculus to the pulvinar in prosimian galagos (Otolemur garnettii) and VGLUT2 staining of the visual pulvinar. J Comp Neurol. 2013; 521(7):1664–1682. [PubMed: 23124867]

Bennett GJ, Nishikawa N, Lu GW, Hoffert MJ, Dubner R. The morphology of dorsal column postsynaptic spinomedullary neurons in the cat. J Comp Neurol. 1984; 224(4):568–578. [PubMed: 6725631]

Bowes C, Burish M, Cerkevich C, Kaas J. Patterns of cortical reorganization in the adult marmoset after a cervical spinal cord injury. J Comp Neurol. 2013; 521(15):3451–3463. [PubMed: 23681952]

Bowes C, Massey JM, Burish M, Cerkevich CM, Kaas JH. Chondroitinase ABC promotes selective reactivation of somatosensory cortex in squirrel monkeys after a cervical dorsal column lesion. Proc Natl Acad Sci U S A. 2012; 109(7):2595–2600. [PubMed: 22308497]

Burton H, Loewy AD. Projections to the spinal cord from medullary somatosensory relay nuclei. J Comp Neurol. 1977; 173(4):773–792. [PubMed: 68038]

Chen LM, Qi HX, Kaas JH. Dynamic reorganization of digit representations in somatosensory cortex of nonhuman primates after spinal cord injury. J Neurosci. 2012; 32(42):14649–14663. [PubMed: 23077051]

Chen S, Aston-Jones G. Evidence that cholera toxin B subunit (CTb) can be avidly taken up and transported by fibers of passage. Brain Res. 1995; 674(1):107–111. [PubMed: 7773677]

Cliffer KD, Giesler GJ Jr. Postsynaptic dorsal column pathway of the rat. III. Distribution of ascending afferent fibers. J Neurosci. 1989; 9(9):3146–3168. [PubMed: 2795158]

Cliffer KD, Willis WD. Distribution of the postsynaptic dorsal column projection in the cuneate nucleus of monkeys. J Comp Neurol. 1994; 345(1):84–93. [PubMed: 8089278]

de Pommery J, Roudier F, Menetrey D. Postsynaptic fibers reaching the dorsal column nuclei in the rat. Neurosci Lett. 1984; 50(1–3):319–323. [PubMed: 6493635]

Dick SH, French AS, Rasmusson DD. Postsynaptic dorsal column and cuneate neurons in raccoon: comparison of response properties and cross-correlation analysis. Brain Res. 2001; 914(1–2):134–148. [PubMed: 11578606]

Enevoldson TP, Gordon G. Postsynaptic dorsal column neurons in the cat: a study with retrograde transport of horseradish peroxidase. Exp Brain Res. 1989a; 75(3):611–620. [PubMed: 2744118]

Enevoldson TP, Gordon G. Spinocervical neurons and dorsal horn neurons projecting to the dorsal column nuclei through the dorsolateral fascicle: a retrograde HRP study in the cat. Exp Brain Res. 1989b; 75(3):621–630. [PubMed: 2744119]

Florence SL, Wall JT, Kaas JH. The somatotopic pattern of afferent projections from the digits to the spinal cord and cuneate nucleus in macaque monkeys. Brain Res. 1988; 452(1–2):388–392. [PubMed: 2456829]

Florence SL, Wall JT, Kaas JH. Central projections from the skin of the hand in squirrel monkeys. J Comp Neurol. 1991; 311(4):563–578. [PubMed: 1721925]

Giesler GJ Jr, Cliffer KD. Postsynaptic dorsal column pathway of the rat. II. Evidence against an important role in nociception. Brain Res. 1985; 326(2):347–356. [PubMed: 3971159]

Giesler GJ Jr, Nahin RL, Madsen AM. Postsynaptic dorsal column pathway of the rat. I. Anatomical studies. J Neurophysiol. 1984; 51(2):260–275. [PubMed: 6323643]

Jain N, Catania KC, Kaas JH. Deactivation and reactivation of somatosensory cortex after dorsal spinal cord injury. Nature. 1997; 386(6624):495–498. [PubMed: 9087408]

Jain N, Florence SL, Qi HX, Kaas JH. Growth of new brainstem connections in adult monkeys with massive sensory loss. Proc Natl Acad Sci U S A. 2000; 97(10):5546–5550. [PubMed: 10779564]

Jain N, Qi HX, Collins CE, Kaas JH. Large-scale reorganization in the somatosensory cortex and thalamus after sensory loss in macaque monkeys. J Neurosci. 2008; 28(43):11042–11060. [PubMed: 18945912]

Kaas JH, Qi HX, Burish MJ, Gharbawie OA, Onifer SM, Massey JM. Cortical and subcortical plasticity in the brains of humans, primates, and rats after damage to sensory afferents in the dorsal columns of the spinal cord. Exp Neurol. 2008; 209(2):407–416. [PubMed: 17692844]

Kaneko T, Fujiyama F. Complementary distribution of vesicular glutamate transporters in the central nervous system. Neurosci Res. 2002; 42(4):243–250. [PubMed: 11985876]

Liao CC, Gharbawie OA, Qi H, Kaas JH. Cortical connections to single digit representations in area 3b of somatosensory cortex in squirrel monkeys and prosimian galagos. J Comp Neurol. 2013; 521(16):3768–3790. [PubMed: 23749740]

Price DD, Mayer DJ. Physiological laminar organization of the dorsal horn of M. mulatta. Brain Res. 1974; 79(2):321–325. [PubMed: 4421432]

Qi HX, Chen LM, Kaas JH. Reorganization of somatosensory cortical areas 3b and 1 after unilateral section of dorsal columns of the spinal cord in squirrel monkeys. J Neurosci. 2011a; 31(38): 13662–13675. [PubMed: 21940457]

Qi HX, Gharbawie OA, Wong P, Kaas JH. Cell-poor septa separate representations of digits in the ventroposterior nucleus of the thalamus in monkeys and prosimian galagos. J Comp Neurol. 2011b; 519(4):738–758. [PubMed: 21246552]

Qi HX, Gharbawie OA, Wynne KW, Kaas JH. Impairment and recovery of hand use after unilateral section of the dorsal columns of the spinal cord in squirrel monkeys. Behav Brain Res. 2013; 252:363–376. [PubMed: 23747607]

Qi HX, Kaas JH, Reed JL. The reactivation of somatosensory cortex and behavioral recovery after sensory loss in mature primates. Front Syst Neurosci. 2014a; 8:84. [PubMed: 24860443]

Qi HX, Reed JL, Gharbawie OA, Burish MJ, Kaas JH. Cortical neuron response properties are related to lesion extent and behavioral recovery after sensory loss from spinal cord injury in monkeys. J Neurosci. 2014b; 34(12):4345–4363. [PubMed: 24647955]

Rexed B. The cytoarchitectonic organization of the spinal cord in the cat. J Comp Neurol. 1952; 96(3): 414–495. [PubMed: 14946260]

Rovo Z, Ulbert I, Acsady L. Drivers of the primate thalamus. J Neurosci. 2012; 32(49):17894–17908. [PubMed: 23223308]

Rustioni A. Non-primary afferents to the cuneate nucleus in the brachial dorsal funiculus of the cat. Brain Res. 1974; 75(2):247–259. [PubMed: 4841918]

Rustioni A. Spinal neurons project to the dorsal column nuclei of rhesus monkeys. Science. 1977; 196(4290):656–658. [PubMed: 404704]

Rustioni A, Hayes NL, O'Neill S. Dorsal column nuclei and ascending spinal afferents in macaques. Brain. 1979; 102(1):95–125. [PubMed: 85470]

Rustioni A, Kaufman AB. Identification of cells or origin of non-primary afferents to the dorsal column nuclei of the cat. Exp Brain Res. 1977; 27(1):1–14. [PubMed: 64365]

Schneider SP. Local circuit connections between hamster laminae III and IV dorsal horn neurons. J Neurophysiol. 2008; 99(3):1306–1318. [PubMed: 18184889]

Sengul, G.; Waston, C.; Tanaka, I.; Paxinos, G. Atlas of the spinal cord of the rat, mouse, marmoset, rhesus, and human. San Diego, CA: Academic Press by Elsevier; 2012. p. 360

Sur M, Nelson RJ, Kaas JH. Representations of the body surface in cortical areas 3b and 1 of squirrel monkeys: comparisons with other primates. J Comp Neurol. 1982; 211(2):177–192. [PubMed: 7174889]

Tandon S, Kambi N, Lazar L, Mohammed H, Jain N. Large-scale expansion of the face representation in somatosensory areas of the lateral sulcus after spinal cord injuries in monkeys. J Neurosci. 2009; 29(38):12009–12019. [PubMed: 19776287]

Vercelli A, Repici M, Garbossa D, Grimaldi A. Recent techniques for tracing pathways in the central nervous system of developing and adult mammals. Brain Res Bull. 2000; 51(1):11–28. [PubMed: 10654576]

Wagman IH, Price DD. Responses of dorsal horn cells of M. mulatta to cutaneous and sural nerve A and C fiber stimuli. J Neurophysiol. 1969; 32(6):803–817. [PubMed: 4981517]

Wang Z, Qi HX, Kaas JH, Roe AW, Chen LM. Functional signature of recovering cortex: Dissociation of local field potentials and spiking activity in somatosensory cortices of spinal cord injured monkeys. Exp Neurol. 2013; 249:132–143. [PubMed: 24017995]

Weng HR, Lenz FA, Vierck C, Dougherty PM. Physiological changes in primate somatosensory thalamus induced by deafferentation are dependent on the spinal funiculi that are sectioned and time following injury. Neuroscience. 2003; 116(4):1149–1160. [PubMed: 12617956]

Willis, WD.; Coggeshall, RE. Structure of the Dordal Horn. In: Willis, WD.; Coggeshall, RE., editors. Sensory Mechnisam of the Spinal Cord. 3. Vol. 1. New York, NY: Kluwer Academic/ PlenumPublishers; 1991. p. 155-184.

Wong-Riley M. Changes in the visual system of monocularly sutured or enucleated cats demonstrable with cytochrome oxidase histochemistry. Brain Res. 1979; 171(1):11–28. [PubMed: 223730]

Xu J, Wall JT. Rapid changes in brainstem maps of adult primates after peripheral injury. Brain Res. 1997; 774(1–2):211–215. [PubMed: 9452211]

Xu J, Wall JT. Functional organization of tactile inputs from the hand in the cuneate nucleus and its relationship to organization in the somatosensory cortex. J Comp Neurol. 1999; 411(3):369–389. [PubMed: 10413773]

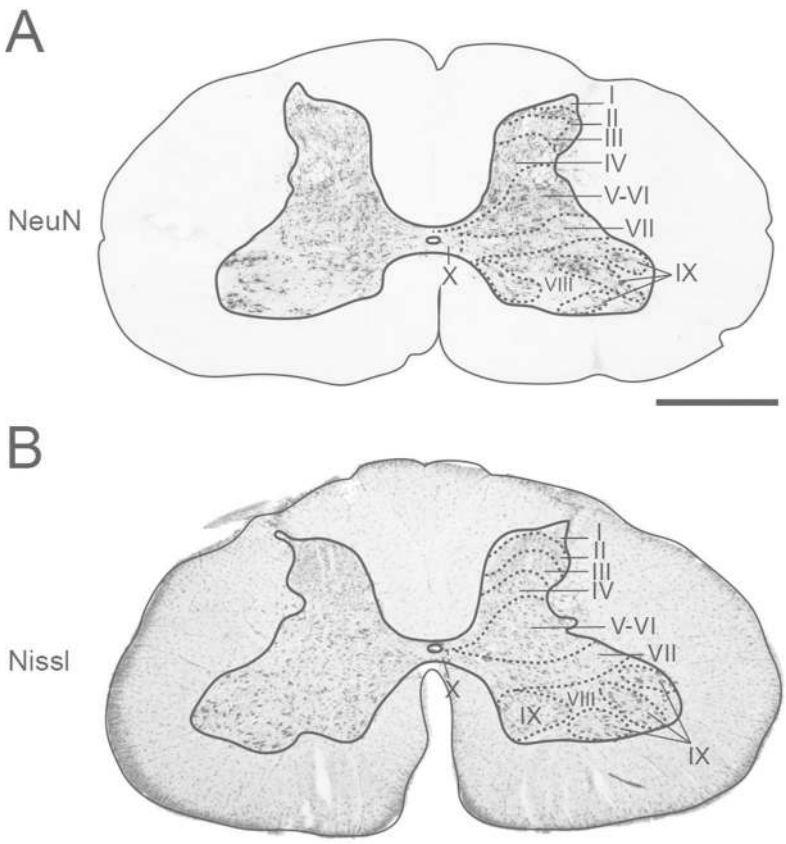

Figure 1.

Transverse sections of the cervical spinal cord (C5) showing the laminae I–X of grey matter with (**A**) NeuN or (**B**) Nissl staining in squirrel monkeys. Laminae follow those portrayed in Sengal et al. (2012). Scale bar is 1 mm.

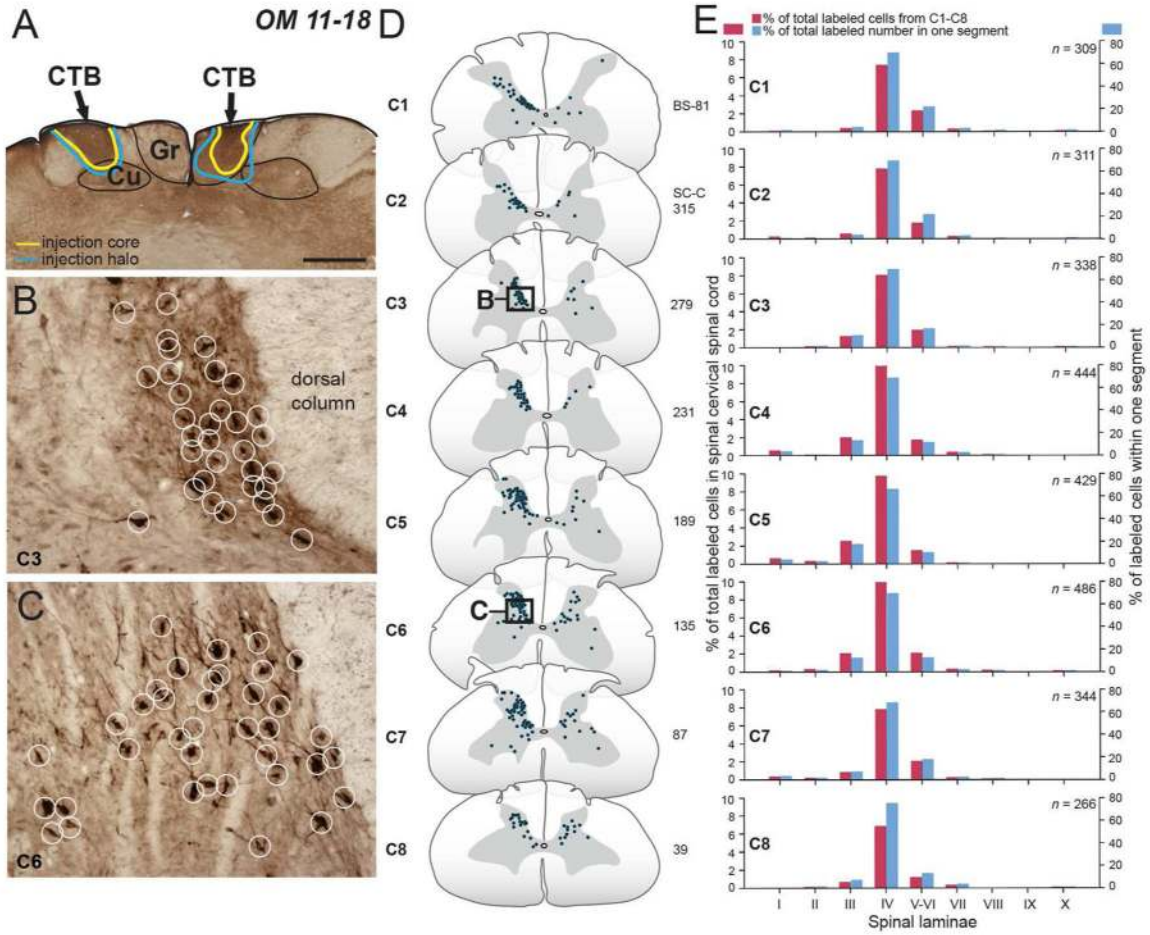

Figure 2.

Distributions of spinal cord neurons labeled by injections of cholera toxin subunit B (CTB) into the dorsal column nuclei of owl monkey 11–18. **A**. CTB was injected into the cuneate nucleus on the left side and the gracile nucleus on the right side. The injection site in the left brainstem also involves the cuneate fasciculus and that in the right side involves the gracile nucleus with some lateral spread into the cuneate nucleus and fasciculus. Yellow and blue lines depict cores and halos of CTB injections. **B**. A large number of CTB-labeled neurons were found in the dorsal horn at a high cervical level C3 (box in **D**). The labeled neurons are marked by white circles. **C.** A large number of CTB-labeled neurons were found in the dorsal horn at a low cervical level C6 (box in **D**). **D.** A great number of CTB-labeled neurons (solid black circles) are primarily distributed in the dorsal horn of cervical spinal cord ipsilateral to the cuneate nucleus injection. A smaller number of CTB-labeled neurons appear on the right side of the cervical spinal cord. **E.** The percentages of the CTB-labeled neurons in laminae I–X across cervical segments C1–C8 ipsilateral to the injection site suggest that the labeled neurons are extensively distributed throughout the cervical spinal cord (red). Within each cervical segment, the CTB-labeled neurons are primarily located in the lamina IV and small numbers of labeled neurons are distributed in laminae V–VI and III (blue; shown as percentages in each segment). "*n*" represents the total number identified in

each segment. Scale bar is 1 mm in **A** and 100 μm in **B**–**C**. Cu, cuneate nucleus; Gr, gracile nucleus.

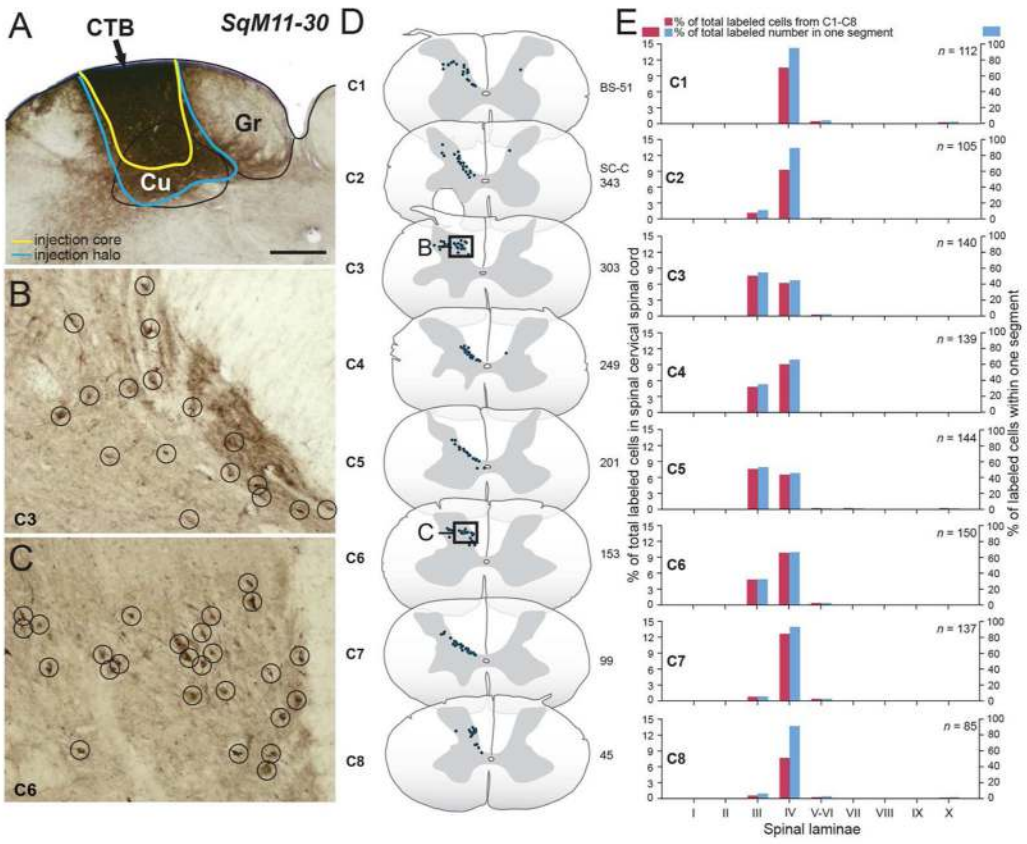

Figure 3.

Distributions of spinal cord neurons labeled by injections of CTB into the cuneate nucleus of squirrel monkey 11–30. **A.** The CTB injection site mainly involves the cuneate nucleus and also the overlying cuneate fasciculus of the left brainstem. **B.** A large number of CTB-labeled neurons are located at a high cervical level C3 (box in **D**). **C.** A comparable number of CTB-labeled neurons are distributed at a low level C6 (box in **D**). **D**. The CTB-labeled neurons are mainly located in the medial aspect of the dorsal horn of the cervical spinal cord ipsilateral to the injection site, with a small number of CTB-labeled neurons on the contralateral side. **E.** The percentages of the CTB-labeled neurons in laminae I–X across cervical segments C1–C8 ipsilateral to the injection site, suggesting labeled neurons were extensively distributed throughout the cervical spinal cord. The CTB-labeled neurons are mainly located in the lamina IV and to a lesser percentage in the lamina III in each segment. Scale bar is 0.5 mm in **A** and 100 μm in **B**–**C**.

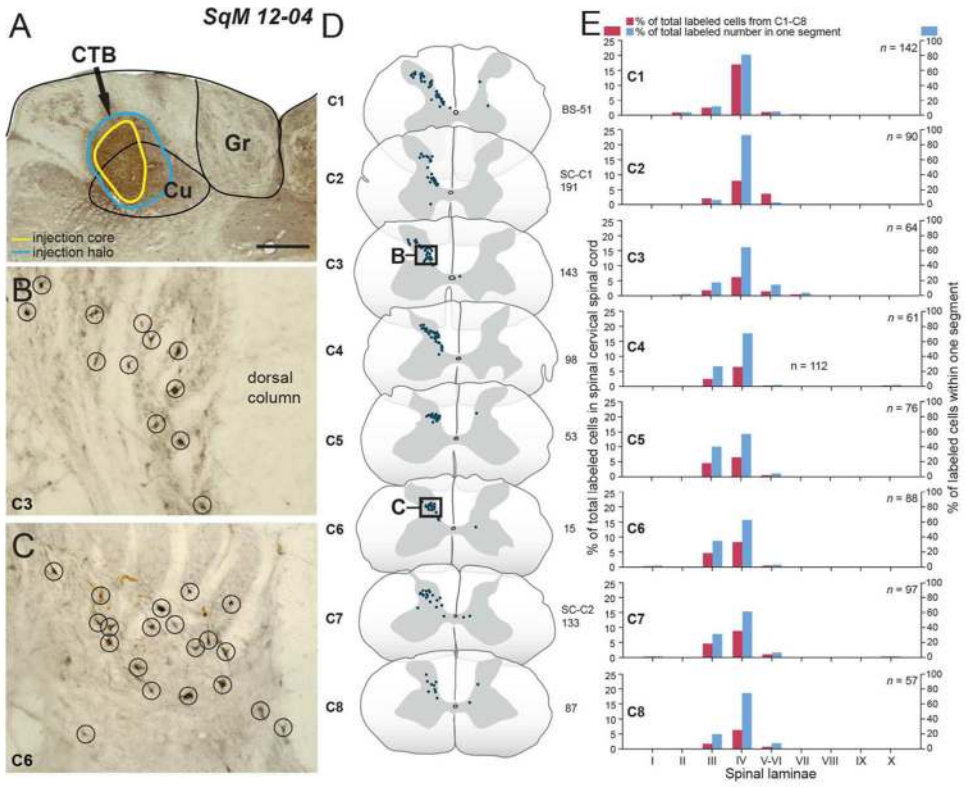

Figure 4.

Distributions of spinal cord neurons labeled by injections of CTB into the cuneate nucleus of squirrel monkey 12-04. **A.** The CTB injection site mainly involves the cuneate nucleus and overlying cuneate fasciculus of the left brainstem. **B.** A large number of CTB-labeled neurons are located at a high cervical level C3 (box in **D**). **C.** A comparable number of CTB-labeled neurons are distributed at a low level C6 (box in **D**). **D.** The CTB-labeled neurons are mainly located in the dorsal horn of the cervical spinal cord ipsilateral to the injection site, with a small number of CTB-labeled neurons on the contralateral side. **E.** The percentages of the CTB-labeled neurons in laminae I–X across cervical segments C1–C8 ipsilateral to the injection site. A great percentage of CTB-labeled neurons are located in the C1 and slightly lesser percentages of CTB-labeled neurons are distributed in C2 to C8. Within each segment, the majority of CTB-labeled neurons are located in the lamina IV and to a lesser percentage in the lamina III. Scale bar is 0.5 mm in **A** and 100 μm in **B**–**C**.

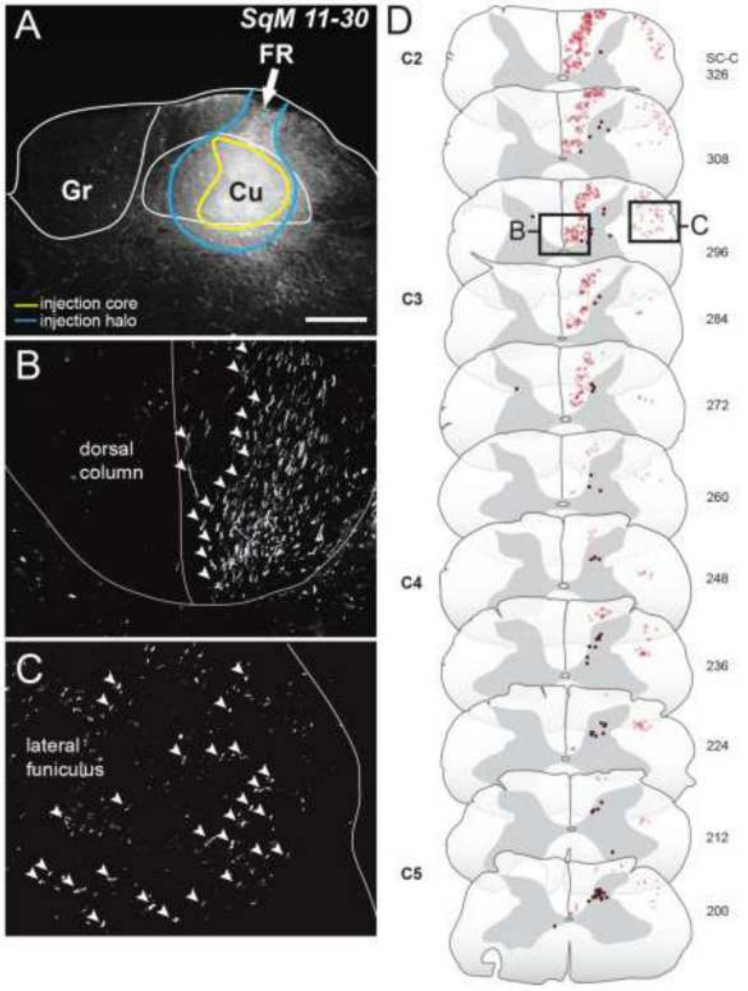

Figure 5.

Locations of axons connecting the cuneate nucleus and cervical spinal cord labeled by injection of fluoro-ruby (FR) into the cuneate nucleus of squirrel monkey 11–30. **A.** The FR injection site is confined to the cuneate nucleus. **B.** A great number of FR-labeled fibers are located across the depth of the cuneate fasciculus (box in **D**). The labeled-fibers are marked by arrowheads. **C.** A small number of FR-labeled fibers are located in the dorsal portion of the lateral funiculus (box in **D**). **D.** The distributions of FR-labeled fibers (red) are mainly in the dorsal column and fewer of them are in the lateral funiculus. The densities of labeled fibers are reduced toward caudal segments from C2 to C5. The FR-labeled neurons are mainly distributed in the dorsal horn of the cervical spinal cord ipsilateral to the injection site, and few of the labeled neurons are located in the contralateral side. Scale bar is 0.5 mm in **A** and 250 μm in **B**–**C**.

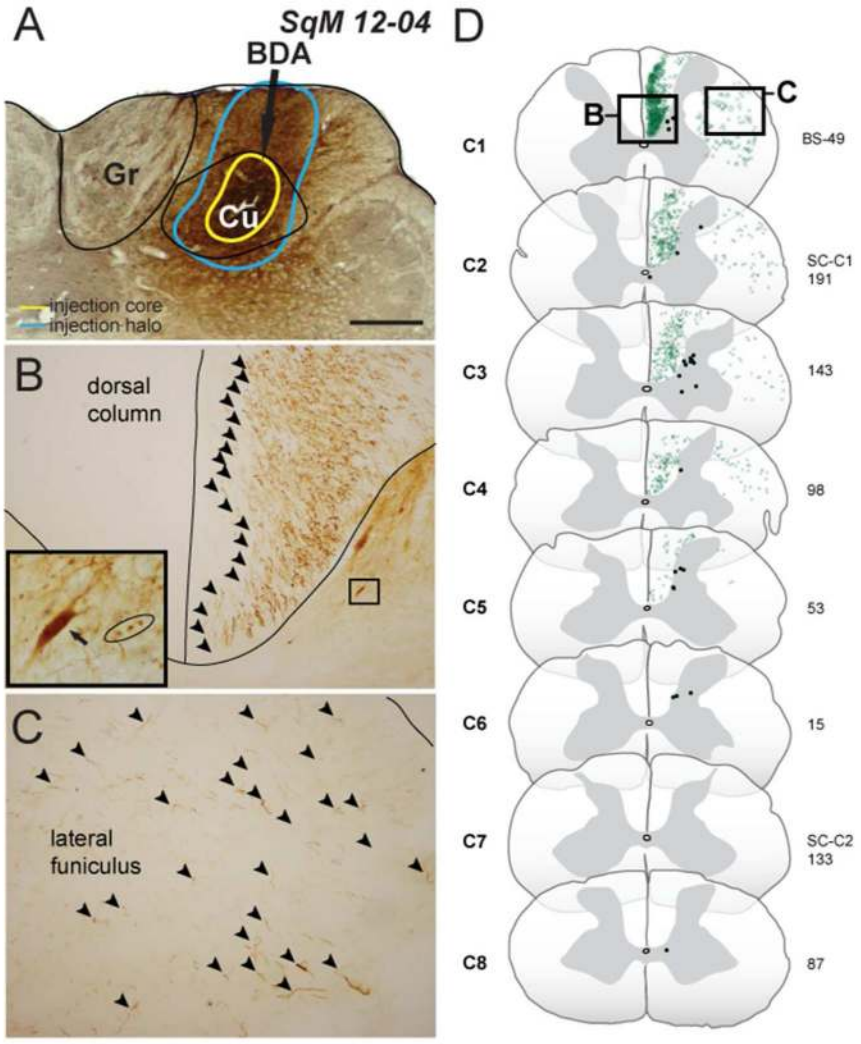

Figure 6.

Locations of axons connecting the cuneate nucleus and cervical spinal cord labeled by injection of biotinylated dextran amine (BDA) into the cuneate nucleus of squirrel monkey 12-04. **A.** The BDA injection site is confined to the cuneate nucleus and the dense uptake zone extends slightly beyond the ventral border of cuneate nucleus. **B.** A large number of BDA-labeled fibers are located across the depth of the cuneate fasciculus (box in **D**). The labeled fibers are marked by arrowheads. The BDA injection labeled cells (arrow in the inset) and axon terminals (black circle in the inset) in the ipsilateral cervical spinal cord. **C.** A small number of BDA-labeled fibers (green) are located dorsally in the lateral funiculus (box in **D**). **D.** The distributions of BDA-labeled fibers are mainly in the cuneate fasciculus and fewer of them are in the lateral funiculus. The densities of labeled fibers are reduced toward caudal segments from C1 to C5. Only a few BDA-labeled neurons are located in the dorsal horn of the cervical spinal cord ipsilateral to the injection site. Scale bar is 0.5 mm in **A**, 250 μm in **B**–**C** and 50 μm in the inset of **B**.

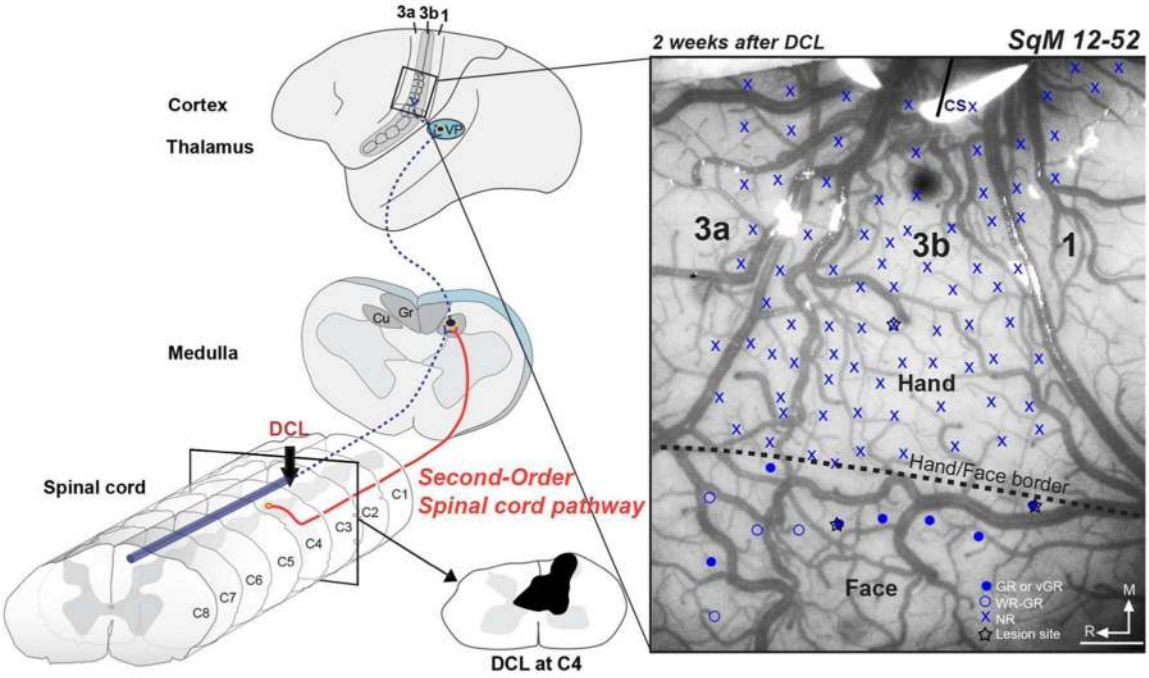

Figure 7.

A complete dorsal column lesion deactivated the contralateral somatosensory cortex of squirrel monkey 12–52. A diagram showing the ascending pathways from the dorsal column and lateral funiculus of spinal cord to the cuneate nucleus in the brainstem, the ventroposterior nucleus (VP) in the thalamus, and up to the primary somatosensory area 3b. Two weeks after a complete dorsal column lesion at the C4 level (shown in black shading), multiunit recordings revealed that neurons throughout the contralateral hand representation of area 3b failed to respond to touches on the hand (penetrations marked with ×). However, neurons in the face representation of area 3b remained responsive. CS, central sulcus; GR, good response; M, medial; NR, no response; R, rostral; WR, weak response; vWR, very weak response. DCL, dorsal column lesion. Scale bar is 1 mm.

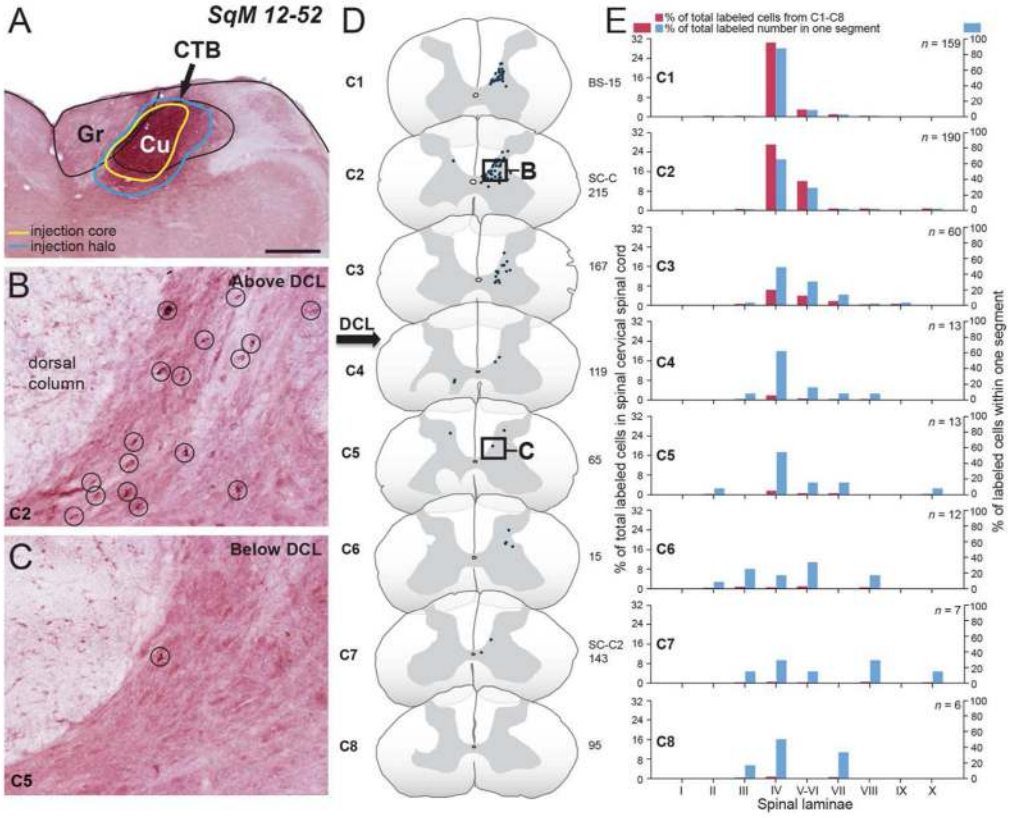

Figure 8.

Distributions of spinal cord neurons labeled by injections of CTB into the cuneate nucleus after a complete dorsal column lesion at C4 of squirrel monkey 12–52. **A.** The CTB injection core site mainly involves the cuneate nucleus with a slight spread beyond the ventral border of cuneate nucleus. **B.** A large number of CTB-labeled neurons are located at a high cervical level C2 (box in **D**). **C.** A small number of CTB-labeled neurons are located at a low level C5 (box in **D**). **D.** Most of the CTB-labeled neurons are located in the dorsal horn of cervical spinal cord C1–C3. Below the dorsal column lesion level, a small numbers of CTB-labeled neurons are scattered in the cervical segments C4–C8. Few CTB-labeled neurons are distributed in the contralateral side. **E.** The percentages of the CTB-labeled neurons in laminae I–X across cervical segments C1–C8 ipsilateral to the injection site. Large percentages of CTB-labeled neurons are in C1 to C3, and significantly reduced percentages of labeled neurons are in C4 to C8 ($p = 0.005$, *t*-test). The CTB-labeled neurons are primarily distributed in the lamina IV, with a lesser amount in lamina V–VI above the lesion level. Below the lesion level, the CTB-labeled neurons tended to locate in the lamina IV but also scattered in other spinal laminae. Scale bar is 0.5 mm in **A** and 100 μm in **B**–**C**.

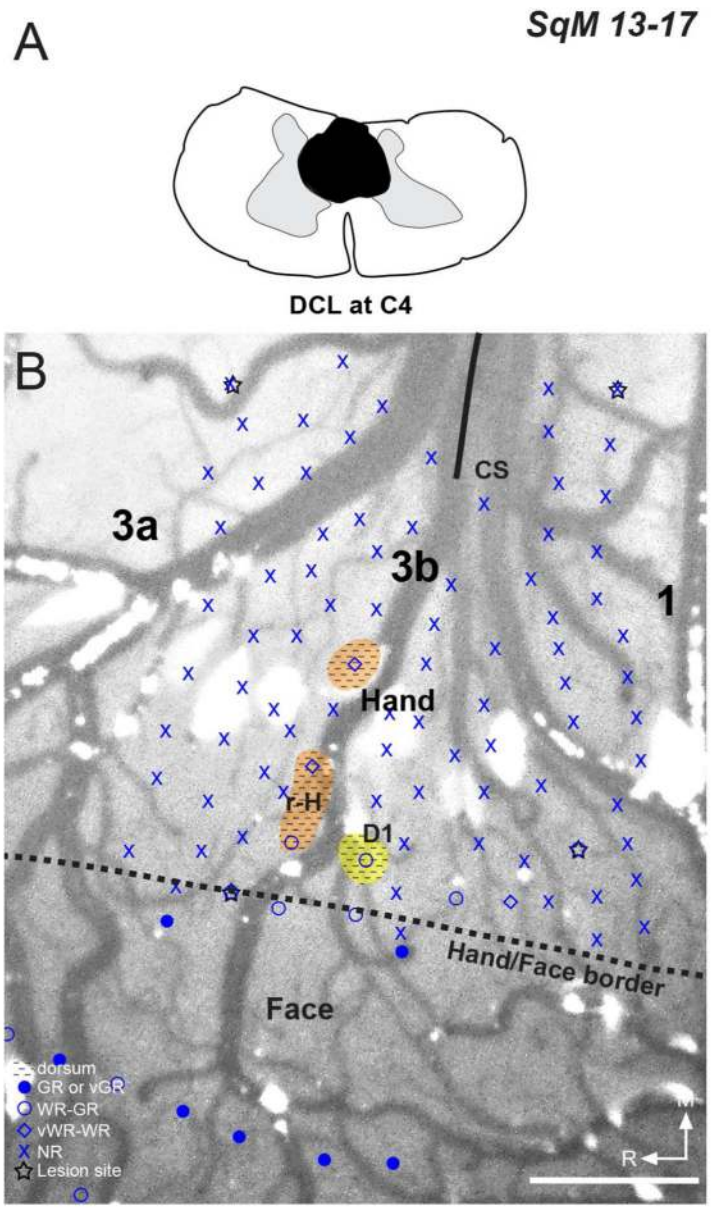

Figure 9.

A nearly complete dorsal column lesion deactivated the contralateral somatosensory cortex of squirrel monkey 13–17. **A.** The lesion site is at C4 in the spinal cord involving most of the right dorsal column, the medioventral region of the left dorsal column, medial regions of the dorsal horn on both sides, and the central canal region. **B.** Two weeks after the lesion, multiunit recording from microelectrode penetrations showing that the majority of neurons in the penetrations in the hand representation were unresponsive to touch. Neurons in 4 penetrations responded to peripheral stimuli with weak responses. The microelectrode penetrations in the face representation detected good or weak responses. The yellow, meshed shading marks a penetration with neurons responsive to hairs on dorsal digit 1, and the orange, meshed shadings mark locations with neurons responsive to hairs on radial hand. Scale bar is 1 mm in **B**. Please see Figure 7 for other conventions.

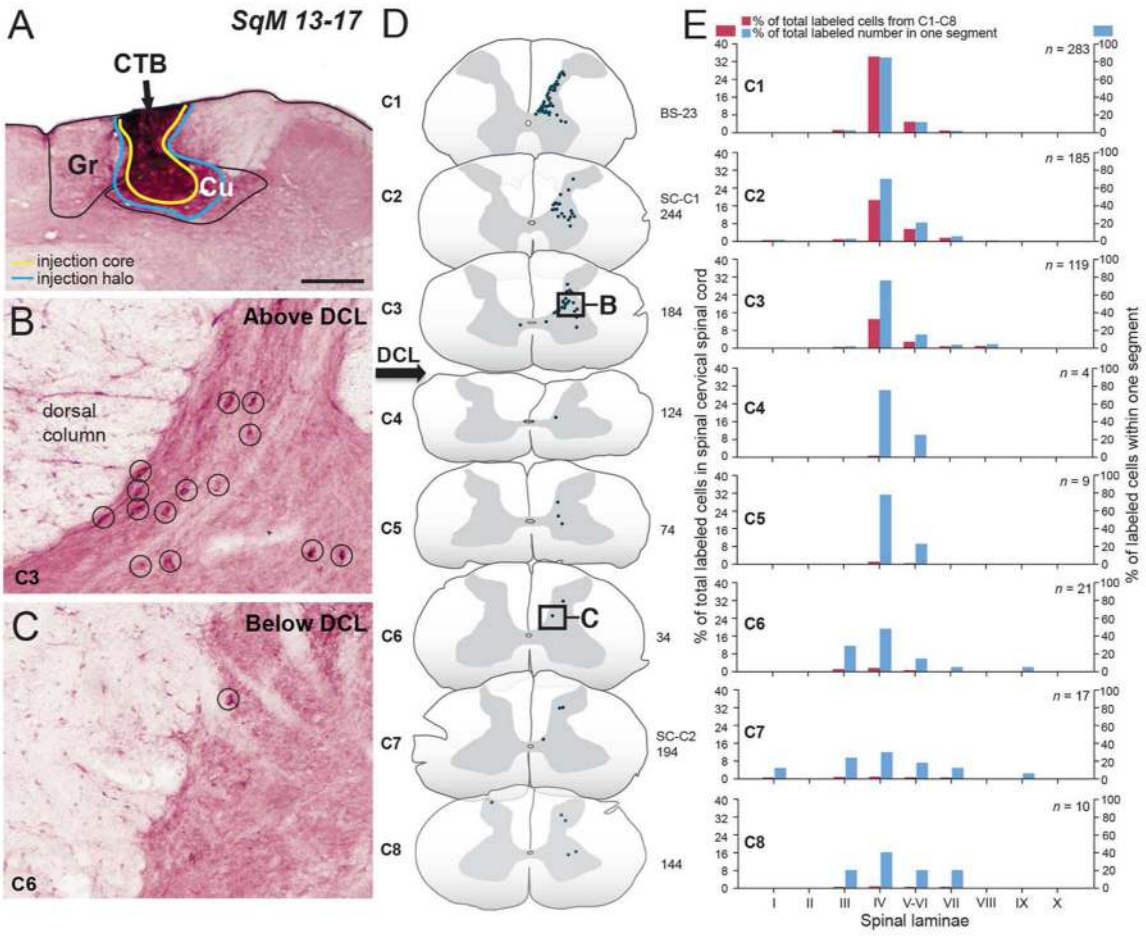

Figure 10.

Distributions of spinal cord neurons labeled by an injection of CTB into the cuneate nucleus after a complete dorsal column lesion at C4 of squirrel monkey 13–17. **A.** The CTB injection core site mainly involves the cuneate nucleus and overlying cuneate fasciculus with a slight spread into the lateral aspect of the gracile nucleus. **B.** A large number of CTB-labeled neurons are located at a high cervical level C3 (box in **D**). **C.** A small number of CTB-labeled neurons are located at a low level C6 (box in **D**). **D.** The majority of CTB-labeled neurons are located in the dorsal horn of cervical spinal cord C1–C3. Below the dorsal column lesion level, a small number of CTB-labeled neurons are scattered in the cervical segments C4–C8. Few CTB-labeled neurons are distributed in the contralateral side. **E.** The percentages of the CTB-labeled neurons in laminae I–X across cervical segments C1–C8 ipsilateral to the injection site. Most CTB-labeled neurons are in C1 to C3. Significantly reduced percentages of labeled neurons are observed in C4 to C8 ($p = 0.002$, *t*-test). The CTB-labeled neurons are primarily distributed in the lamina IV, to a lesser amount in the lamina V–VI above the lesion level. Below the lesion level, the CTB-labeled neurons are mainly located in the lamina IV but are also in other spinal laminae. Scale bar is 0.5 mm in **A** and 100 μm in **B**–**C**.

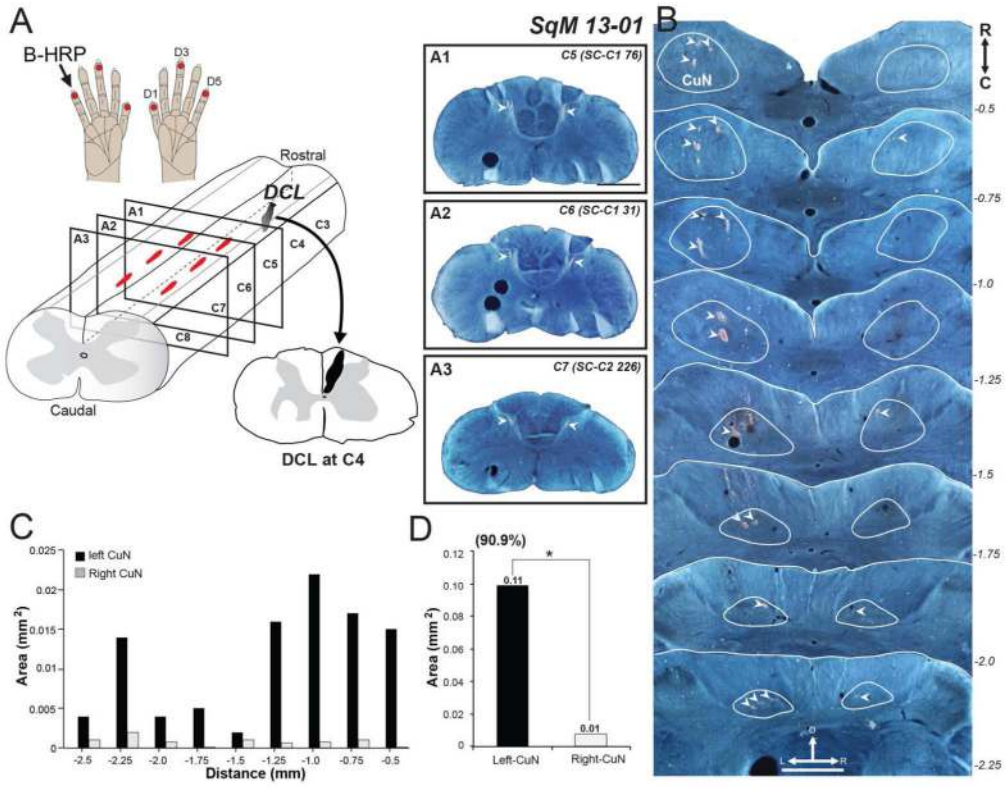

Figure 11.

Terminations of peripheral afferents in the dorsal horn of spinal cord and cuneate nucleus in the brainstem after an incomplete lesion of the right cuneate fasciculus in squirrel monkey 13-01. Terminations of primary afferents in the cuneate nucleus were revealed by choleratoxin subunit B conjugated with wheat germ agglutinin-horseradish peroxide (B-HRP) injections into distal digits 1, 3 and 5 of both hands. **A.** The B-HRP-labeled axonal terminals are located in the dorsal horn of C5, C6 and C7 on the two sides (**A1**, **A2** and **A3**; white arrowheads), corresponding to the peripheral inputs from digits 1, 3 and 5. The lesion site at C4 of the right side was restricted to the area between the posterior median sulcus and the posterior intermediate sulcus to the bottom of the dorsal column, which mainly involved the cuneate fasciculus. **B.** Photomicrographs showing the B-HRP-labeled axonal terminals (white arrowheads) form patches in the cuneate nucleus of the left brainstem throughout rostrocaudal sections. Small foci of B-HRP labeled terminals are scattered in the cuneate nucleus on the right side. **C.** Bar graphs showing the total surface area of B-HRP labeled foci at caudal to rostral levels relative to the obex in the cuneate nucleus on the left (black) and right (gray) sides. The values of distance are measured in millimeters caudally (negative numbers) in reference to the obex. **D.** The B-HRP labeled area on the lesioned side (0.01 mm_2) of the cuneate nucleus is significantly less than the labeled area on the control side (0.11 mm_2; $p < 0.001$, *t*-test), indicating an estimated completeness of 91% of dorsal column lesion (consistent with the estimate from transverse sections through the lesion site). Scale bar is 1 mm in **A1**–**A3** and is 1 mm in **B**.

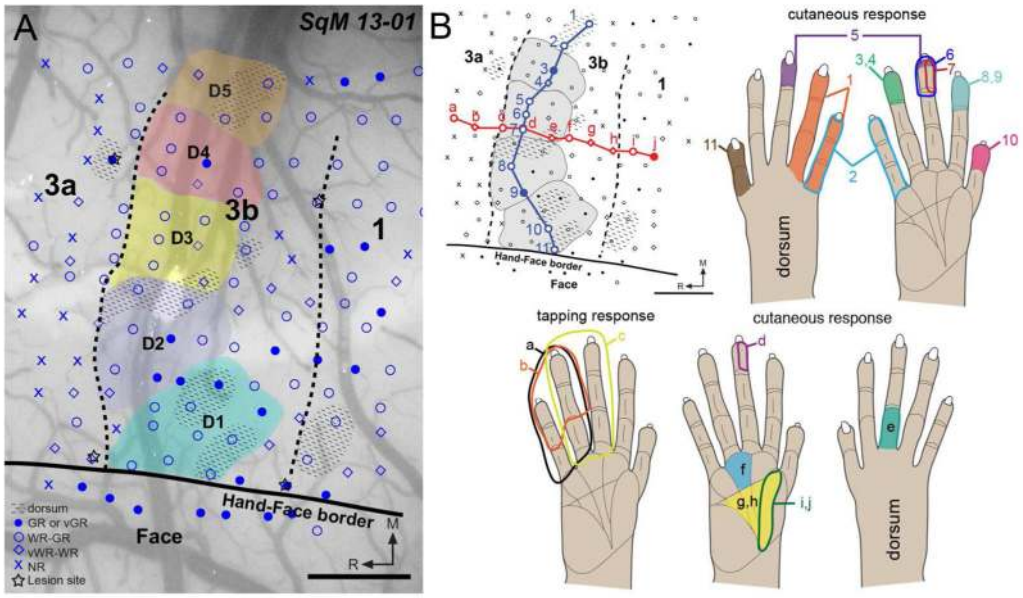

Figure 12.

Microelectrode multiunit recordings in the area 3b and adjoining areas 3a and 1 contralateral to the dorsal column lesion of squirrel monkey 13-01. **A.** In the hand representations, most electrode penetrations had neurons with weak or very weak responses to peripheral stimuli although few of them had neurons with good responses. A few penetrations had unresponsive neurons. The representations of digits 1–5 (outlined colored regions) were arranged in a normal mediolateral arrangement. The palm representation was located caudal to the digit representations. Penetrations within territories marked by meshed shading had neurons with receptive fields on the dorsal hairy hand. Others were on the glabrous hand. All penetrations in the face representation had neurons with very good or good responses. **B.** Examples of shifts of receptive fields along the mediolateral (letters) and rostrocaudal (numbers) rows of recording sites (red & blue). Scale bar is 1 mm in **A**. Please see Figure 7 for other conventions.

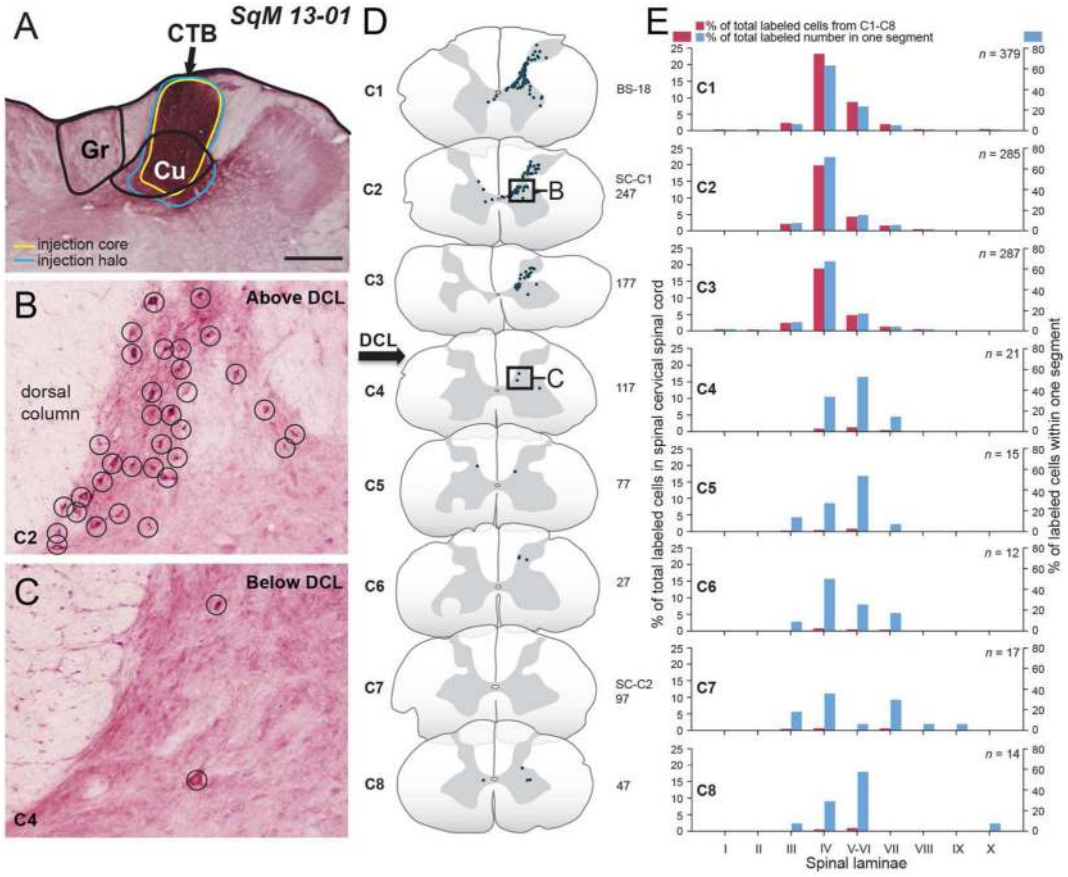

Figure 13.

Distributions of spinal cord neurons labeled by injections of CTB into the cuneate nucleus after a complete dorsal column lesion at C4 of squirrel monkey 13-01. **A.** The CTB injection core site mainly involves the cuneate nucleus and overlying cuneate fasciculus. The dense uptake zone slightly spreads beyond the ventral border of cuneate nucleus. **B.** A great number of CTB-labeled neurons are located at a high cervical level C2 (box in **D**). **C.** A small number of CTB-labeled neurons are located below the lesion level C4 (box in **D**). **D.** The majority of CTB-labeled neurons are concentrated in the dorsal horn of cervical spinal cord C1–C3. A small number of CTB-labeled neurons are scattered in the cervical segments C4–C8 below the level of lesion. A few CTB-labeled neurons are distributed on the contralateral side. **E.** The percentages of the CTB-labeled neurons in laminae I–X across cervical segments C1–C8 ipsilateral to the injection site. Large percentages of CTB-labeled neurons are in C1 to C3. Significantly reduced percentages of labeled neurons are observed in C4 to C8 ($p < 0.001$, *t*-test). The CTB-labeled neurons are primarily distributed in the lamina IV, and to a lesser amount in lamina V–VI and III above the lesion level. Below the lesion level, the CTB-labeled neurons are mainly located in lamina V–VI and IV but are also scattered in other spinal laminae. Scale bar is 0.5 mm in **A** and 100 μm in **B**–**C**.

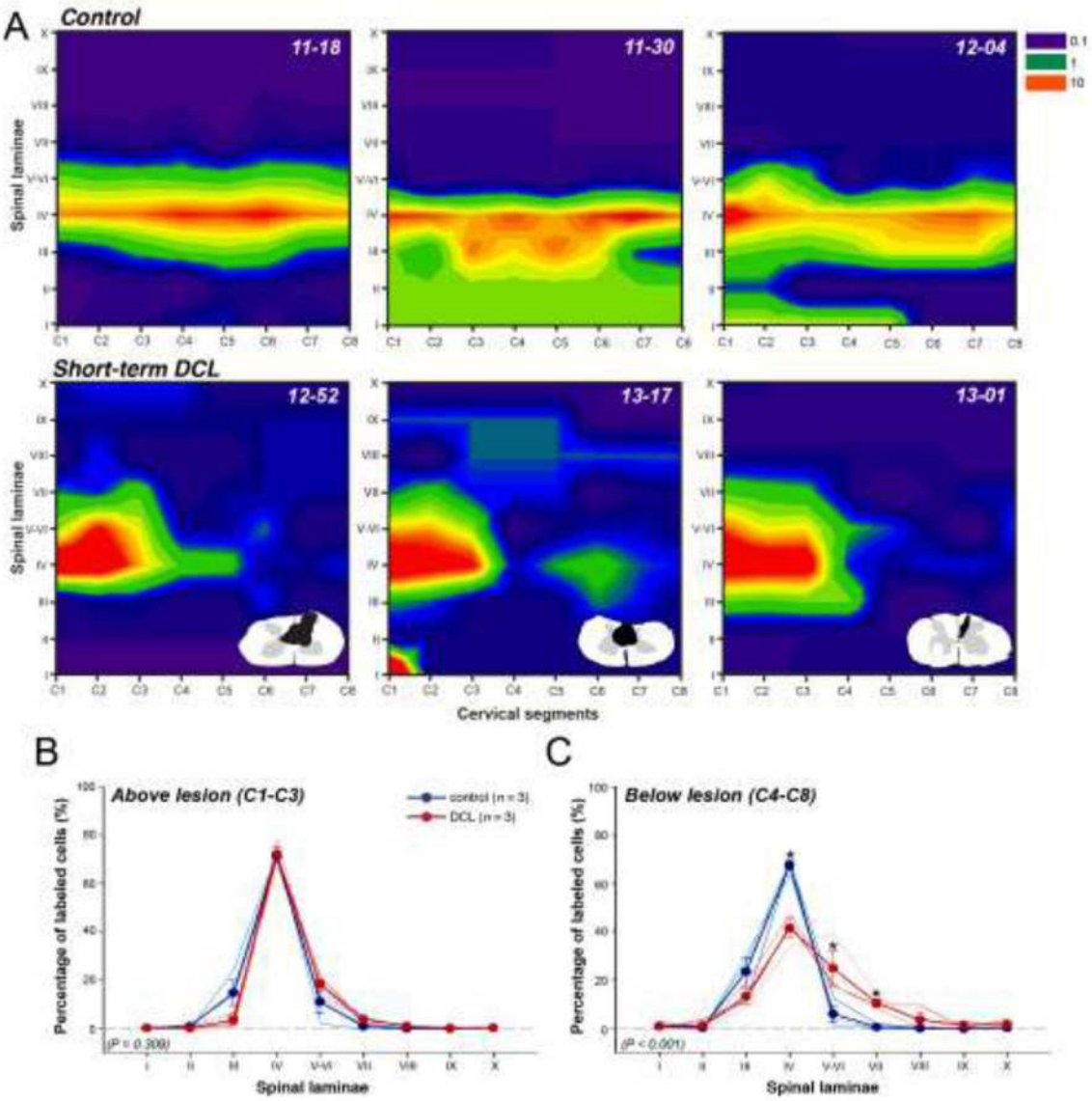

Figure 14.

Summary of locations of spinal cord neurons labeled by the injections of CTB into the dorsal column nuclei in normal ($n = 3$) and dorsal column lesioned monkeys ($n = 3$). **A.** 2D heatmaps showing that the majority of CTB-labeled neurons are located in the lamina IV throughout the cervical spinal cord in normal monkeys. In the three dorsal column lesioned monkeys, the CTB-labeled neurons are concentrated in the lamina IV of C1 to C3. Small percentages of CTB-labeled neurons remain below the level of lesion C4 to C8. **B.** Comparisons of the percentages of labeled neurons in laminae I–X of C1–C3 above the lesion between the control and dorsal column lesion cases. The dorsal column lesion did not alter the laminar distributions ($p = 0.309$, Two Way Anova). **C.** Comparisons of the percentages of labeled neurons in laminae I–X of C4–C8 that are below the lesion between the two groups. The dorsal column lesions altered the overall distributions in laminae I–X ($p < 0.001$, Two Way Anova with *post hoc* Student-Newman-Keul Method). Although the

percentages of labeled neurons remain high in the lamina IV, the percentages of labeled neurons in laminae IV is significantly reduced below the lesion. This allows the small number of neurons in lamina V–VI and VII to be proportionately significantly greater. Data in **B** and **C** are presented by mean ± SEM. * $p < 0.05$.

Table 1

Table of Primary Antibody Used

Primary antibody antigen	Immunogen	Details	Concentration
NeuN	Purified cell nuclei from mouse brain	Millipore, Billerica, MA; mouse monoclonal (Cat#: MAB377); RRID: AB_2298772	1:5000
vesicular glutamate transporter 2 (VGLUT2)	Recombinant protein from rat VGLUT2	Millipore, Billerica, MA; mouse monoclonal (Cat#: MAB5504); RRID: AB_262186	1:5000